WIND TUNNEL AND FLIGHT TEST INVESTIGATION OF THE CESSNA 140 FOR CORRELATION OF AERODYNAMIC DERIVATIVES

BY

R. A. BOYD
LCDR., U.S. NAVY

R. L. BOTHWELL
LT., U.S. NAVY

PRINCETON UNIVERSITY

AERONAUTICAL ENGINEERING LABORATORY

REPORT NO. 179

WIND TUNNEL AND FLIGHT TEST INVESTIGATION OF THE CESSNA 140 FOR CORRELATION OF AERODYNAMIC DERIVATIVES

Thesis
B79

TABLE OF CONTENTS

Object:

The object of this investigation was to examine the correlation between the static stability and control aerodynamic derivatives obtained from wind tunnel tests of an unpowered model of a light airplane with the same derivatives obtained from flight tests of the full scale airplane. The airplane investigated was the Cessna 140.

Summary:

The aerodynamic characteristics of the Cessna 140 were obtained from tests of an unpowered 1/10 scale model in the Princeton University Atmospheric Wind Tunnel. These characteristics were reduced from data obtained from the six component balance system of this tunnel during a normal series of test runs. The same aerodynamic characteristics were measured on the full scale airplane, owned by the Department of Aeronautical Engineering, from a program of flight tests for its performance and its stability characteristics using methods suggested in references 2 and 3. The results indicate that the performance and handling qualities of light airplanes can be predicted from wind tunnel tests of small scale, unpowered models with adequate accuracy. These tests also demonstrated the effectiveness of steady state flight techniques to obtain many of the important stability and control derivatives.

Date and Place of Investigation

This study was conducted during the period extending from January to June 1951 and made use of the facilities and equipment of the Aeronautical Engineering Department.

I INTRODUCTION

The aerodynamic design development of modern aircraft usually proceeds in three distinct phases. These phases are: analytical treatment from a preliminary three view, wind tunnel tests of the most promising design, and finally flight test analysis of the full scale airplane. The methods for proper development from stage to stage have been carefully studied for high performance aircraft with a great deal of information available on correlating these various stages. It has been found that large scale-powered model tests of a particular airplane design adequately predicts, with only a few limitations, the actual performance and handling qualities of the prototype airplane. For this reason all designs of high performance aircraft count heavily on information obtained in the wind tunnel phase.

The light airplane designer, on the contrary, usually advances from the analytical study phase to the final design without any recourse to wind tunnel model study at all, due in large measure to the expense involved in the development of models and the high cost of wind tunnel time. Tests of large scale, powered models are therefore practically unknown in the development of the light airplane.

It was felt that a study of the accuracy with which the results of inexpensive wind tunnel tests of a small scale, unpowered model could predict the performance and flying qualities of a typical light airplane would be of considerable interest to the light plane industry, and eventually point the way to considerable improvement in this class of airplane.

The airplane used for this study was the Cessna 140, a typical two place personal airplane in the light category. A 1/10 scale model of

this airplane was constructed and tested, unpowered, in the atmospheric wind tunnel in the Aeronautical Engineering Department at Princeton University. The results of these tests were analyzed by conventional means for their aerodynamic characteristics. At the same time actual flight tests of the Cessna 140 were conducted which yielded the same information at full scale. The major purpose of this study was the correlation of these results.

Flight test information required to correlate the results discussed above were obtained from previously conducted flight programs, Ref. 4 through 7, as well as additional tests made by the authors to obtain aerodynamic data otherwise unavailable.

A secondary purpose of this investigation was to study the steady state methods of flight testing discussed in Ref. 2 and 3. These methods can yield many of the important aerodynamic characteristics of the airplane without recourse to the expensive and laborious methods, now in great favor, involving frequency or transient response techniques.

II SYMBOLS

a_o	Two-dimensional slope of lift curve (per degree)
a_w	Slope of the lift curve of the wing (per degree)
A	Wing aspect ration
b	Airplane wing span (feet)
C_D	Airplane Drag Coefficient
C_{D_α}	Slope of the curve of drag coefficient vs. angle of attack
C_L	Lift coefficient (per degree)
C_{L_α}	Slope of Lift Coefficient vs. Angle of Attack Curve
C_n	Yawing moment coefficient
$C_{n_{\delta_a}}$	Yawing moment coefficient due to aileron deflection (per degree)
$C_{n_{\delta_r}}$	Yawing moment coefficient due to rudder deflection (per degree)
C_l	Rolling moment coefficient
$C_{l_{\delta_a}}$	Rolling moment coefficient due to aileron deflection (per degree)
$C_{l_{\delta_r}}$	Rolling moment coefficient due to rudder deflection (per degree)
C_{n_β}	Yawing moment coefficient due to sideslip (per degree)
$C_{n_{\delta_r}}$	Yawing moment coefficient due to rudder deflection (per degree)
$C_{n_{\delta_a}}$	Yawing moment coefficient due to aileron deflection (per degree)

C_y	Side force coefficient
$C_{y_{\delta r}}$	Side force coefficient due to rudder deflection (per degree)
C_{y_β}	Side force coefficient due to sideslip (per degree)
C_m	Pitching moment coefficient
C_{m_δ}	Pitching moment coefficient due to elevator deflection (per degree)
f	Equivalent parasite drag area = C_D S
L	Rolling moment (ft. lbs.)
l_t	Airplane tail length (ft.)
N	Yawing moment (ft. lbs.)
q	Dynamic pressure (lb./ft.^{2})
S	Area (sq. ft.)
V	Airplane velocity (ft./sec.)
W	Gross weight (lbs.)
α	Angle of attack (degrees)
β	Angle of sideslip (degrees)
δ_r	Rudder deflection (degrees)
δ_a	Aileron deflection (degrees)
Δ	increment of

$\frac{d\delta_r}{d\beta}$ Slope of rudder deflection vs. sideslip curve

$\frac{d\delta_a}{d\beta}$ Slope of aileron deflection vs. sideslip curve

η_t Tail efficiency factor

η_v Vertical tail efficiency factor

ϕ Angle of bank (degrees)

ψ Angle of yaw (degrees)

Sign Convention

Left rudder angle is positive

Right aileron up is positive

Sideslip with wind coming in from the right is positive

Right angle of bank is positive

III LIST OF FIGURES AND ILLUSTRATIONS

15. Pitching Moment Coefficient versus Lift Coefficient with Flaps Deflected -- wind tunnel test.
16. Determination of Neutral Points -- wind tunnel tests.
17. Pitching Moment Coefficient versus Elevator Deflection for various Lift Coefficients -- wind tunnel test.
18. Elevator Power versus Lift Coefficients -- wind tunnel and flight test.
19. Drag Polar -- wind tunnel and flight test.
20. Photograph of the Cessna 140 Model in the Wind Tunnel Test Section.
21. Photograph of the Cessna 140 full scale Airplane as instrumented for flight test.
22. Photograph of the Cessna 140 Airplane in flight towing drogue used to determine Rudder Power.

IV EQUIPMENT AND PROCEDURE

A. Wind Tunnel Test Program

The wind tunnel, located at the Princeton University Aeronautical Engineering Laboratory, is of the single return closed-throat type with a 3.5 x 5 foot test section. The hydraulic pneumatic balance system measures lift, drag, side force, as well as pitching, rolling, and yawing moments relative to the wind axis of the tunnel. The model was mounted in the test section on two faired supports attached to the wing, in addition to a tail jack. The tail jack length was adjusted to vary the angle of attack of the model. The support system was mounted on a turntable which could be rotated to selected angles of yaw. Fig. 20 is a photograph showing the model mounted in the test section.

The model of the Cessna 140 was to a scale of ten to one. The fuselage was constructed of solid balsa sections; while the wing and tail surfaces were of mahogany. Flap, aileron, rudder and elevator deflections were adjustable. The surface finish was a polished lacquer. No propeller was used in the tests.

All forces and moments were measured relative to the wind axis of the tunnel at a dynamic pressure of 24.4 lbs. per sq. ft. The test on the inverted model at negative angles of attack established that the flow inclination in the tunnel test section was insignificant; so this was neglected throughout the data reduction. Thus, the longitudinal data was measured relative to the "stability" axes after wind tunnel wall corrections were made to drag and to angle of attack.

The lateral data was converted to the "stability" axes by applying the pertinent trigonometric function of the angle of yaw.

As pointed out in Ref. 12, wind tunnel test data is normally presented relative to the "stability" axes, although flight measurements and observations are made relative to the airplane body axes. Since these wind tunnel results were to be compared with flight test values the data was converted to the airplane body axes by applying trigonometric functions of the angle of attack.

All pitching, yawing and rolling moments were then transferred from the pivot axis to the airplane center of gravity position at 27.7% m.a.c. on the thrust line.

No Reynold's Number corrections were made, since maximum lift coefficient and minimum drag coefficient were not needed for this investigation, and the effect of Reynold's Number on stability and control derivatives is small.

B. Flight Test Program

1. Equipment

Although both lateral and longitudinal stability parameters were investigated in the wind tunnel, the authors of this report conducted flight tests for lateral information only because longitudinal derivatives were available from previous steady state flight tests of the same airplane, Ref. 4 through Ref. 7. All flight tests were conducted at a constant indicated airspeed of 103 mph at about 1500 ft. altitude with the airplane in a straight sideslip, at different angles of sideslip. Although it would have been desirable to check the lateral derivatives at various airspeeds, friction in the yaw vane prevented slower speed tests, and the power limitations of the Cessna 140 made faster speeds impracticable. The recorded data

included a protractor reading of angle of bank, autosyn readings of sideslip angle, rudder, and aileron deflections. Tests were repeated with flaps fully deflected.

In order to correctly analyze the flight test data it was necessary to maintain a nearly constant value of the tail efficiency factor, which is dependent upon thrust coefficient. This was accomplished by maintaining constant power settings for all test flights and losing altitude, if necessary, to hold constant indicated airspeed. All flight tests were made just after sunrise because of the calm atmospheric conditions existing at that time. It was found that any wind or thermal air currents tended to cause excessive scatter of the observed data.

The airplane tested was the Cessna 140, NX89207, a single engine, high wing, two place, personal type monoplane with external bracing and fixed, conventional landing gear. The wing is rectangular with rounded tips. It has the normal configuration, single vertical tail, Freise type ailerons, and is equipped with trailing edge, plain flaps. The airplane is of semi-monocoque, all metal construction, except the wings which are fabric covered. All control surfaces are metal. Fig. 21 is a photograph showing the appearance of the airplane as instrumented for these flight tests. The general specifications and dimensions as given by drawings and reports of the manufacturer are included as Appendix I.

2. Instrumentation

The airspeed was measured with a standard sensitive type airspeed indicator connected to a full swiveling pivot static head attached to a boom extending one chord length ahead of the leading edge of the starboard wing. This instrument was calibrated by means of the speed course method.

The yaw meter was attached to the port wing with a boom extending one chord length ahead of the leading edge. The yaw vane was geared to a 24 volt, 400 cycle autosyn transmitter. The autosyn follower was calibrated to give angle of yaw in degrees.

The rudder and aileron deflections were measured by the same type of autosyn transmitters, linked to the respective control cables. The autosyn followers were calibrated to give rudder and aileron deflection in degrees.

The angle of bank was measured in degrees with a propeller protractor placed on a level section of the cabin floor.

3. Theory of Steady State Flight Testing for Lateral Derivatives

The solution of the lateral static stability derivatives by straight sideslip tests is simply based on the steady state equations of lateral motion:

$$\text{(a)}\ C_{Y_\beta}\cdot\beta - C_L\frac{V}{g}\dot{\psi} + C_L\phi + C_{Y_{\delta_r}}\delta_r = 0$$

(1) $$\text{(b)}\ C_{l_\beta}\cdot\beta + C_{l_r}\frac{b}{2V}\dot{\psi} + C_{l_{\delta_a}}\cdot\delta_a + C_{l_{\delta_r}}\delta_r = 0$$

$$\text{(c)}\ C_{n_\beta}\cdot\beta + C_{n_r}\frac{b}{2V}\dot{\psi} + C_{n_{\delta_r}}\cdot\delta_r + C_{n_{\delta_a}}\cdot\delta_a = 0$$

When the airplane is flown along a straight flight path, by reference to a directional gyro or distant horizon point, the rate of yaw equals zero ($\dot{\psi}=0$), and the above equations become:

$$\text{(a)}\ C_{Y_\beta}\cdot\beta + C_L\phi + C_{Y_{\delta_r}}\cdot\delta_r = 0$$

(2) $$\text{(b)}\ C_{l_\beta}\cdot\beta + C_{l_{\delta_a}}\cdot\delta_a + C_{l_{\delta_r}}\cdot\delta_r = 0$$

$$\text{(c)}\ C_{n_\beta}\cdot\beta + C_{n_{\delta_r}}\cdot\delta_r + C_{n_{\delta_a}}\cdot\delta_a = 0$$

For a selected sideslip angle, these equations establish the amount of bank and lateral controls required to maintain zero yaw rate.

By differentiating equations (2), the lateral static stability derivatives are obtained in terms of the control derivatives, lift coefficient, and the slopes of the bank and control angle curves relative to the sideslip angle.

$$(3)\quad \begin{aligned} (a)\quad -C_{Y_\beta} &= C_L\left(\frac{d\phi}{d\beta}\right) + C_{Y_{\delta_r}}\left(\frac{d\delta_r}{d\beta}\right) \\ (b)\quad -C_{\ell_\beta} &= C_{\ell_{\delta_a}}\left(\frac{d\delta_a}{d\beta}\right) + C_{\ell_{\delta_r}}\left(\frac{d\delta_r}{d\beta}\right) \\ (c)\quad -C_{n_\beta} &= C_{n_{\delta_r}}\left(\frac{d\delta_r}{d\beta}\right) + C_{n_{\delta_a}}\left(\frac{d\delta_a}{d\beta}\right) \end{aligned}$$

While flying the Cessna 140 in a steady sideslip and maintaining zero yaw rate, the control angles and angle of bank were recorded. This procedure was repeated at various angles of sideslip, flaps up and flaps down, to determine the δ_a, δ_r and ϕ curves of Fig. 6 and Fig. 7.

The static derivatives could now be solved from equation (3) when the control derivatives had been determined.

4. Aileron Control Derivatives

The aileron control power was computed from the aileron deflection necessary to balance an applied rolling moment. A steel bar, three feet long with a cross section of 2.25 sq. in., was attached to the starboard wing at the outboard strut attachment fittings. A light wooden bar of identical shape was similarly attached to the port wing. The net weight of 29 lbs. acting at 8.917 ft. lateral distance from the airplane centerline produced an applied rolling moment of 266 ft. lbs. Flights with the wing weight were then performed in the same manner as before. The difference

in aileron angles, $\Delta \delta_a = 1.40°$, between test flights with and without the applied rolling moment as shown in Fig. 8, determines the aileron power.

For the small angles of bank required at the tested sideslip angles, the cos ϕ has been assumed unity; so, the applied rolling moment coefficient may be derived as:

$$L_a = W_a \cdot y$$

$$Cl_a = W_a \cdot y / qsb = .0188$$

From equation (2)(b), the equilibrium in roll can be expressed as:

(1) $C_{l_\beta} \cdot \beta_1 + C_{l_{\delta_a}} \cdot \delta_{a_1} + C_{l_{\delta_r}} \cdot \delta_{r_1} + C_{l_a} = 0$ (with weight)

(2) $C_{l_\beta} \cdot \beta_2 + C_{l_{\delta_a}} \cdot \delta_{a_2} + C_{l_{\delta_r}} \cdot \delta_{r_2} = 0$ (without weight)

By subtracting (2) from (1) at the same angles of sideslip ($\beta_1 = \beta_2$):

(3) $C_{l_{\delta_a}} \cdot \Delta \delta_a + C_{l_{\delta_r}} \cdot \Delta \delta_r + C_{l_a} = 0$

The difference in rudder deflection, $\Delta \delta_r$, necessary to balance any adverse yaw caused by $\Delta \delta_a$ was not measurable. Therefore $C_{n_{\delta_a}}$ was assumed equal to zero: $C_{n_{\delta_a}} = - C_{n_{\delta_r}} \left(\frac{\Delta \delta_r}{\Delta \delta_a} \right) = 0$

Equation (3) becomes: $C_{l_{\delta_a}} = - \frac{C_{l_a}}{\Delta \delta_a} = .0013$

5. Rudder Control Derivative

The rudder control power was computed from the rudder deflection necessary to balance an applied yawing moment created by towing a drogue from the starboard wing. The drogue used for the applied yawing moment consisted of a conventional airport wind sock made of canvas, with the small end constricted by a draw string in order to obtain the required drag force. The large end was secured to a heavy wire hoop, to which the light woven wire tow cable was

attached. This cable was led through a pulley fair-lead secured to the after strut attachment, thence to the fuselage side near the door. At this point the cable was attached to a steel ring, which in turn was mounted on a bracket riveted to the fuselage skin. Four strain gages were mounted on the steel ring (two in tension and two in compression) with the terminals wired into a bridge circuit in the cabin. An ammeter connected in the bridge circuit was calibrated to read the drag force of the towed wind sock. The equivalent parasite drag area of the drogue was measured in the wind tunnel and verified in flight by the strain gage equipment ($f = 1.91$). This drag acting at the lateral distance from the airplane centerline created an applied yawing moment of 453 ft. lb. The straight sideslip tests were then conducted with the drogue streamed. At the termination of this test, the drogue was jettisoned in flight and the straight sideslip runs without the applied yawing moment were repeated to verify previously obtained data. The rudder angles for test flights with and without the applied moment have been plotted on Fig. 9. The $\Delta\delta_r$ was 3.05 degrees with respect to the gliding flight test. Because of the additional drag force of the drogue, it was found necessary to glide in order to keep an η_v of about unity at the tail and still maintain the test airspeed.

From equation (2)(c), the equilibrium in yaw can be written as:

(1) $C_{n_\beta} \cdot \beta_1 + C_{n_{\delta_r}} \cdot \delta_{r_1} + C_{n_{\delta_a}} \cdot \delta_{a_1} + C_{n_a} = 0$ (with drogue)

(2) $C_{n_\beta} \cdot \beta_2 + C_{n_{\delta_r}} \cdot \delta_{r_2} + C_{n_{\delta_a}} \cdot \delta_{a_2} = 0$ (without drogue)

As with the rolling equations, subtracting (2) from (1) at the same sideslip angles gives:

(3) $C_{n_{\delta_r}} \cdot \Delta\delta_r + C_{n_{\delta_a}} \cdot \Delta\delta_a + C_{n_a} = 0$

The aileron difference, $\Delta \delta_a$, necessary to balance any rolling moment caused by the difference in rudder deflections, $\Delta \delta_r$, between runs with and without the drogue was not detectable. Therefore, $C_{l_{\varepsilon_r}}$ was assumed equal to zero. $C_{l_{\varepsilon_r}} = - C_{l_{\delta_a}} \left(\frac{\Delta \delta_a}{\Delta \delta_r} \right) = 0$

$$C_{n_a} = \frac{fY}{Sb} = .0032$$

Equation (3) becomes:

$$C_{n_{\varepsilon_r}} = - \frac{C_{n_a}}{\Delta \delta_r} = -.0010$$

The importance of towing the drogue at the same power as in the straight sideslip tests and gliding to maintain the test airspeed can be seen from Fig. 9; for only 2.0 degrees of $\Delta \varepsilon_r$ was required in the full throttle, 80% rated power, tow flight in which altitude was maintained. This apparent increase of η_v from 1.0 to 1.5 was partially due to greater slipstream velocity at the tail caused by the 30% power increase required to tow the drogue at 103 mph. However, a larger factor was the greater twist of the slipstream at the higher power setting. This effect of the slipstream, evident under conditions of high power at relatively slow speed, must be offset by more right rudder. So, when the drogue was towed from the starboard wing in level flight at full throttle, less left rudder was required to prevent yaw rate. Thus, the smaller value of $\Delta \delta_r$, due primarily to the increased twist of the slipstream, would cause the incorrect calculation of a high value of $C_{n_{\delta_r}}$. Although this change in slipstream effect with power could be determined by towing successively from each wing, the simpler solution is to keep the same power settings while losing altitude to maintain speed.

With the primary rudder control power determined, the secondary rudder derivative was estimated by the simple geometric relationship:

$$C_{Y_{\delta_r}} = -\frac{b}{\ell_v} C_{n_{\delta_r}} = .0025$$

Equations (3) were then solved for the side force derivative, dihedral effect, and directional stability.

All flight tests were repeated in order to establish the reproducibility of results.

V RESULTS

The curves of flight test and wind tunnel data of the Cessna 140, from which the stability derivatives have been obtained, are plotted on Fig. 1 through Fig. 19. For ease of comparison, the static stability and control derivatives from both test mediums have been listed in Table I, shown on Page 18.

For the comparison of flight test to wind tunnel determined derivatives, the tail efficiency factor, η_V, of the Cessna 140 in level flight at 103 mph has been estimated at unity; the η_V of the propellerless model, .90. Both of these assumptions are considered reasonable and will be used throughout the discussion. For comparison purposes, the lateral static derivatives determined from wind tunnel angles of attack of zero and ten degrees have been interpolated to the flight test angle of attack of 3.35 degrees. This interpolated increment was small in every case.

A. The Lateral Aerodynamic Derivatives

1. The Aileron Control Derivatives

The predicted $C_{l_{\delta_a}}$ from the wind tunnel tests as shown in Fig. 4 was 29% too high. This is no reflection on the use of powerless models, for the ailerons are clear of the propeller effect. Furthermore, Ref. 10, a report which compares the $pb/2V$ values from the wind tunnel and flight tests of numerous aileron and wing configurations, states that "the aileron effectiveness developed in flight may be considerably less than that theoretically predicted on the basis of aileron characteristics measured in the wind tunnel, presumably because of wing twisting and deflections in the aileron control system." It is further stated that one degree of wing twist would reduce apparent aileron effectiveness by about 20%.

Table I

Comparison of Static Stability and Control Derivatives from Wind Tunnel and Flight Test Data

LATERAL DERIVATIVES

Flaps Up

derivative	Wind Tunnel $\alpha = 0$	Wind Tunnel $\alpha = 10°$	Wind Tunnel Interpolated $\alpha = 3.35°$	Flight Test
C_{Y_β}	-.0075	-.0075	-.0075	-.0080
C_{l_β}	-.0010	-.0010	-.0010	-.0013
C_{n_β}	.00042	.00066	.00043	.00042
$C_{l_{\delta a}}$	.0020	.0017	.0019	.0013
$C_{n_{\delta r}}$	-.00085	-.000846	-.000846	-.0010
$C_{l_{\delta r}}$	0	-.0002	negligible	0
$C_{n_{\delta a}}$	-.00006	-.00027	-.00013	0
$C_{Y_{\delta r}}$	.0021	.0022	.0022	.0025

Flaps Down

derivative	Wind Tunnel $\alpha = 0$	Wind Tunnel $\alpha = 10°$	Wind Tunnel Interpolated $\alpha = 3.35°$	Flight Test
C_{Y_β}	-.0075	-.0072	-.0074	-.0089
C_{l_β}	-.0010	-.0010	-.0010	-.0013
C_{n_β}	.00046	.00057	.00050	.00039

LONGITUDINAL DERIVATIVES

C_{m_δ}	-.0128 (at C_L = .373)	-.01335	See Fig. 18
Neut. Pt.	.366c	.376c	
C_{L_α} and C_{D_α}	See Drag Polar, Fig. 19.		

The adverse yaw, $C_{n_{\delta_a}}$, was predicted as -.0001.per degree from the wind tunnel test and this value is negligibly small. The flight test value was too small to measure and was assumed zero.

2. The Rudder Control Derivatives

$C_{n_{\delta_r}}$ measured in the wind tunnel was -.0008. Corrected for η_v this becomes -.0009 or just 10% smaller than the flight test value of -.0010.

The wind tunnel $C_{Y_{\delta_r}}$ was .0022, Fig. 5, and was 12% smaller than the flight test value of .0025. A weighted correction for η_v would further reduce this error.

Values of $C_{\ell_{\delta_r}}$ for both test mediums were negligible.

3. The Side Force Derivative

From equation (3)(a):

$$-C_{Y_\beta} = C_L \cdot \frac{d\varphi}{d\beta} + C_{Y_{\delta_r}} \cdot \frac{d\xi_r}{d\beta}$$

the flaps up flight test value was:

$$C_{Y_\beta} = -.0080$$

the flaps down flight test value was:

$$C_{Y_\beta} = -.0089$$

These side force derivatives were just 6% and 15% higher respectively than the wind tunnel C_{Y_β} of -.0075 from Fig. 3. The side force on the propeller and the additional slipstream velocity on the vertical tail in powered flight account basically for this difference. When the flaps are lowered, this derivative increases because of the Y component of the force due to slipstream on the flaps. Although side force derivative is not a critical design parameter, it is noted that the wind tunnel test of the unpowered model gave a small error in C_{Y_β} in the predicted direction.

4. Dihedral Effect

From equation (3)(b):

$$-C_{l_\beta} = C_{l_{\delta a}} \frac{\partial \delta_a}{\partial \beta} + C_{l_{\delta r}} \frac{d\delta r}{\partial \beta}$$

The flaps up flight test value was:

$$C_{l_\beta} = -.0013$$

The flaps down flight test value was:

$$C_{l_\beta} = -.0014$$

The above indicated increase in dihedral effect with flap deflection is contrary to the known condition in that the downwind flap is more immersed in the propeller slipstream and so exerts a greater rolling moment, tending to reduce the dihedral effect. In the flight test, as seen from the above equations, the aileron deflection necessary to balance the dihedral rolling moment with sideslip was the primary measure of the dihedral effect. However, the effectiveness of the aileron on the downwind side in the straight sideslip test was evidently decreased because of an interference from the adjacent lowered flap. It seems logical that this interference increased linearly with sideslip angle. Therefore, the aileron deflection slope with flaps deflected was probably increased because of less aileron effectiveness and not more dihedral effect. In view of this evident blocking of the aileron, the flight tested C_{l_β} with flaps deflected should be re-examined.

The value of C_{l_β} from the wind tunnel test curves of Fig. 2 is -.0010. Although 23% below the flight test value, the actual difference in effective dihedral is very small. To illustrate this, a small change in wing tip shape would cause a percentage change in effective dihedral of 30%. The dihedral actually measured on the test airplane was 1.3°, and not the one degree shown on the blueprints from which the model was constructed.

From these results it can be concluded that the dihedral effect in the critical high speed region, where danger of oscillation exists, can be

adequately predicted from the wind tunnel tests of an unpowered model. To insure positive dihedral effect in the landing configuration, careful calculation will be required to prevent misleading results.

5. Directional Stability

From equation (3)(c)

$$-C_{n_\beta} = C_{n_{\varepsilon_r}} \cdot \frac{d\varepsilon_r}{d\beta} + C_{n_{\delta_a}} \cdot \frac{d\delta_a}{d\beta}$$

The flight test value with flaps up:

$$C_{n_\beta} = .00042$$

The flight test value with flaps down:

$$C_{n_\beta} = .00039$$

In the flaps up condition, the wind tunnel test $C_{n_\beta} = .00043$ had only 3% more directional stability than the Cessna 140 in flight at 103 mph. Although this discrepancy is small, two corrections should be made. First, the correction for η_v of the tail would further raise the effective of the model to .00048. Second, the destabilizing directional effect of the propeller would have the following effect, as calculated from Ref. 11:

$\Delta(C_{n_\beta})_{T=0}$ = destabilizing effect of the propeller at zero thrust

$$\Delta(C_{n_\beta})_{T=0} = \frac{-\pi D^2 \ell_p \left(\frac{dC_{Yp}}{d\chi}\right) N}{4 S_w b} = -.00006$$

To correct to 60% rated power:

$$\Delta(C_{n_\beta}) = 1.3\, \Delta(C_{n_\beta})_{T=0} = -.00008$$

Therefore, the corrected wind tunnel test $C_{n_\beta} = .00040$.

The flight test value of C_{n_β} with flaps down decreased because of the directionally destabilizing force of the propeller slipstream on the downwind flap when the model is tested at an angle of yaw.

Corrections to the wind tunnel, flaps down value of C_{n_β} are:

Tail efficiency factor correction:

$$(C_{n_\beta})_{\eta_v=1.0} = \frac{(C_{n_\beta})_{\eta_v=.9}}{.9} = .00055.$$

Propeller correction for full throttle:

$$\Delta C_{n_\beta} = 1.5\ \Delta (C_{n_\beta})_{T=0} = -.00009.$$

Therefore, the corrected wind tunnel test $C_{n_\beta} = .00046.$

This corrected value of flaps down C_{n_β} is 18% higher than the corresponding flight test value. This difference is important, for even though Dutch Roll characteristics make directional stability most important in the high speed range, high C_{n_β} greatly improves the handling qualities in the landing configuration. So, as with the dihedral effect, corrections should be made for the destabilizing slipstream force on the down flaps.

B. The Longitudinal Derivatives

1. C_{L_α} and C_{D_α}

As expected, the slope of the lift and drag curves from the wind tunnel tests shown in Fig. 10 checked closely with flight test data. Drag polars from the wind tunnel and the flight test of the Cessna 140 reported in Ref. 7 have been plotted on Fig. 19 for graphic comparison of C_{L_α} and C_{D_α}.

The analytical calculation of C_{L_α} gives:

$$a_w = \frac{1}{1 + \frac{57.3\, a_0}{\pi A}} = .081$$

This excellent correlation of the unpowered model tests verified that power effects have little influence on C_{L_α} and C_{D_α}.

2. Elevator Control Power

The power effects on longitudinal stability and elevator power have been a major argument for use of powered models in wind tunnel tests. In Ref. 4, the elevator power of the Cessna 140 was accurately determined by steady state flight tests.

In Fig. 18 both flight test and wind tunnel test values of C_{m_δ} have been plotted versus C_L. At the equilibrium lift coefficient of .373 corresponding to the wind tunnel dynamic pressure of 24.4 lbs/ft^2, the flight test determined $C_{m_\delta} = -.0133$. This corresponds closely to the wind tunnel $C_{m_\delta} = -.0128$. Although the increase in C_{m_δ} with power at lower speeds can be quite accurately predicted, good elevator design should be based on the value of C_{m_δ} without power effects. With this consideration and the close correlation of elevator power for the two test mediums when η_v approaches unity, it appears reasonable to conclude that the wind tunnel test data of an unpowered model is well suited for accurate elevator design. A slightly more conservative C_{m_δ} would result if a windmilling propeller were used on the model and allowance made for ground effect of the landing approach.

3. Stick-Fixed Stability

The important longitudinal stability characteristic known as stick-fixed stability was obtained from the wind tunnel tests by the Schuldenfrei method of determining the neutral point. This technique, described in Ref. 9, is based on the premise that $dC_m/dC_L = C_m/C_L$ at the neutral point. In Fig. 15 the neutral point has been graphically determined at 36.6% m.a.c. with flaps up and 36.5% m.a.c., flaps down. Methods of correcting the stability criterion for the destabilizing effects of power are described at length in Ref. 11.

For light planes such effects will not exceed more than one or two percent. In fact, from the steady state flight tests of the Cessna 140 reported in Ref. 5, the stick-fixed neutral point was determined at 37.6% m.a.c. for a glide condition and at 36.6% m.a.c. for normal cruise.

From the above comparison of the longitudinal stability and control parameters it is seen that excellent correlation between wind tunnel and flight tests was achieved. Thus it appears reasonable to conclude that the horizontal stabilizer and the elevator can be designed for optimum longitudinal stability from the wind tunnel tests of an unpowered model.

VI CONCLUSIONS

This investigation has shown that the aerodynamic derivatives determined from wind tunnel tests of a 1/10 scale unpowered model of the Cessna 140 check closely the derivatives obtained from the flight tests of the full scale airplane, as seen in Table I. It should be noted that the wind tunnel results listed in Table I are uncorrected for slipstream velocity or power effects and that these predictable corrections bring the values to very close agreement.

These tests indicate that the rudder and elevator power can be accurately predicted from unpowered model tests, but confirmed the previous NACA finding that the wind tunnel value of aileron effectiveness is too high. The correlation of the static stability derivatives was excellent. Although the percentage difference in dihedral effect was large, the magnitude of this difference was small.

In view of these results, it is concluded that careful analysis of wind tunnel tests of a small scale, unpowered model will predict the flying qualities of a light airplane.

The reproducibility and consistency of the results obtained from the steady state flight tests indicate that this method can be used with good success for determining static stability and control derivatives. Also, it seems advisable that this method should be used in conjunction with frequency response techniques for the more accurate solution of the dynamic derivatives.

VII RECOMMENDATION

It is recommended that light plane manufacturers consider the utilization of wind tunnel tests of small scale, unpowered models for predicting and improving the flying qualities of new designs.

VIII REFERENCES

1. Perkins, Courtland D., and Hage Robert E., "Airplane Performance Stability and Control", John Wiley & Sons, Inc., New York, Second Printing, March, 1950.

2. Perkins, Courtland D., "Methods for Obtaining Aerodynamic Data Through Steady State Flight Testing, Part I, The Longitudinal Derivatives", Aeronautical Engineering Laboratory, Princeton University, 1950.

3. Perkins, Courtland D., "Methods For Obtaining Aerodynamic Data Through Steady State Flight Testing, Part II, The Lateral Derivatives". Aeronautical Engineering Laboratory Report No. 170, Princeton University.

4. Livingston, William H., "Determination of the Elevator Power and the Damping in Pitch of the Cessna 140 Airplane from Flight Tests", Aeronautical Engineering Laboratory Report No. 160, Princeton University.

5. Graham, Dunstan, "Longitudinal Stability and Control Flight Tests of the Cessna 140 Airplane", Aeronautical Engineering Laboratory Report No. 111, Princeton University.

6. "Flight Test Laboratory Tests on Cessna 140", by Aeronautical Engineering Class of 1951, Aeronautical Engineering Laboratory Report No. 166, Princeton University.

7. Polve, James H., "Correlation of Performance Data on the Cessna 140 Airplane", Aeronautical Engineering Laboratory Report No. 173, Princeton University.

8. LaCouture, J. E., "Flight Study of the Improvement in Directional Stability and Damping in Yaw of an F4U-5 Airplane through an Automatically Controlled Servo Rudder", Aeronautical Engineering Laboratory Report No. 162, Princeton University.

9. Schuldenfrei, Marvin, "Some Notes on the Determination of the Stick-Fixed Neutral Point from Wind-Tunnel Data", N.A.C.A. RB 3120 (WR L-344), September, 1943.

10. Gilruth, R. R., and Turner, W. N., "Lateral Control Required for Satisfactory Flying Qualities Based on Flight Tests of Numerous Airplanes", N.A.C.A. Report No. 715, 1941.

11. Ribner, H. S., "Notes on the Propeller and Slipstream in Relation to Stability", N.A.C.A. WR L-25, 1944.

12. Kayten, G. G., "Analysis of Wind-Tunnel Stability and Control Tests in Terms of Flying Qualities of Full-Scale Airplanes", N.A.C.A. Report No. 825, 1945.

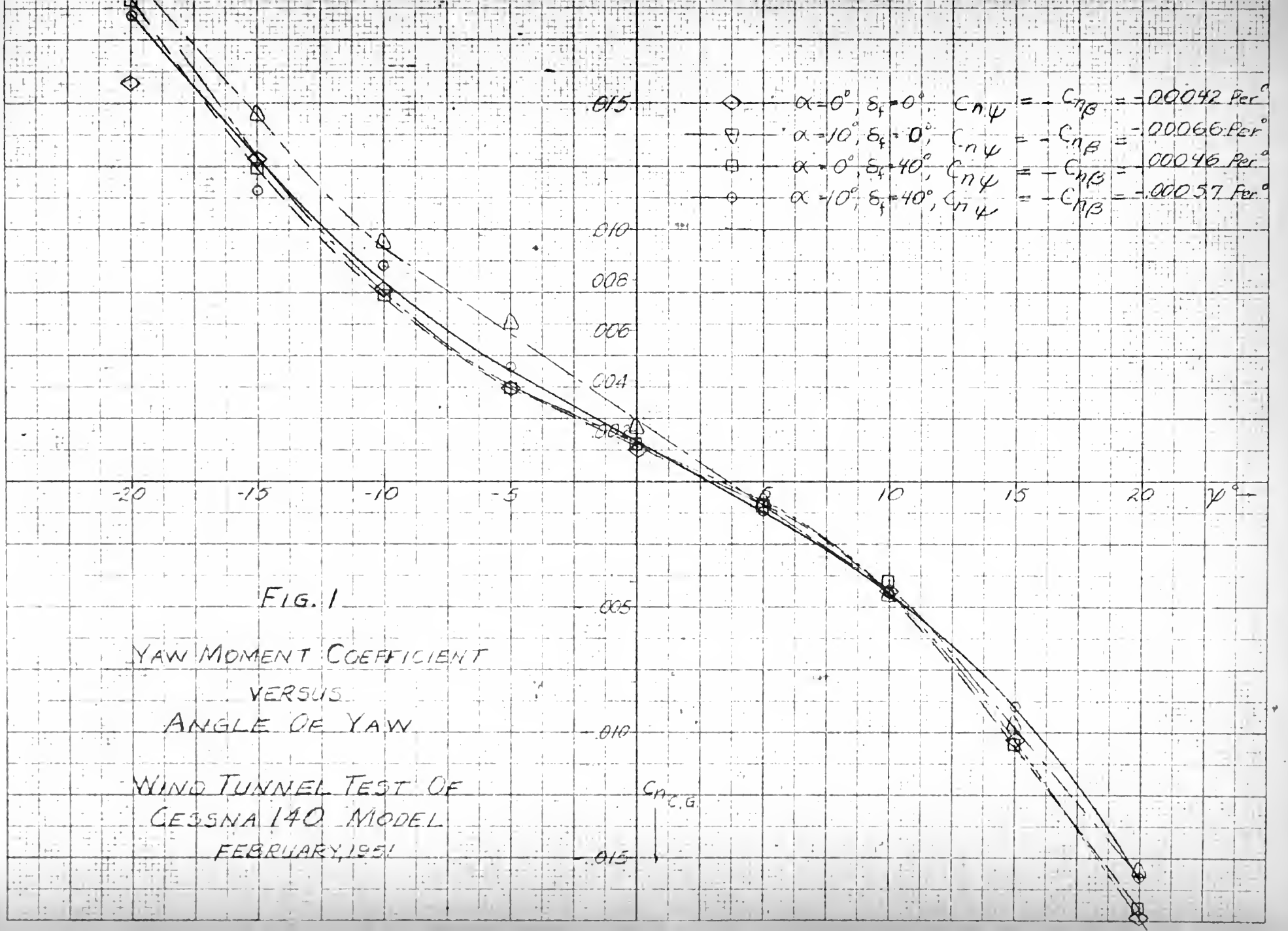

FIG. 1

YAW MOMENT COEFFICIENT
VERSUS
ANGLE OF YAW

WIND TUNNEL TEST OF
CESSNA 140 MODEL
FEBRUARY, 1951

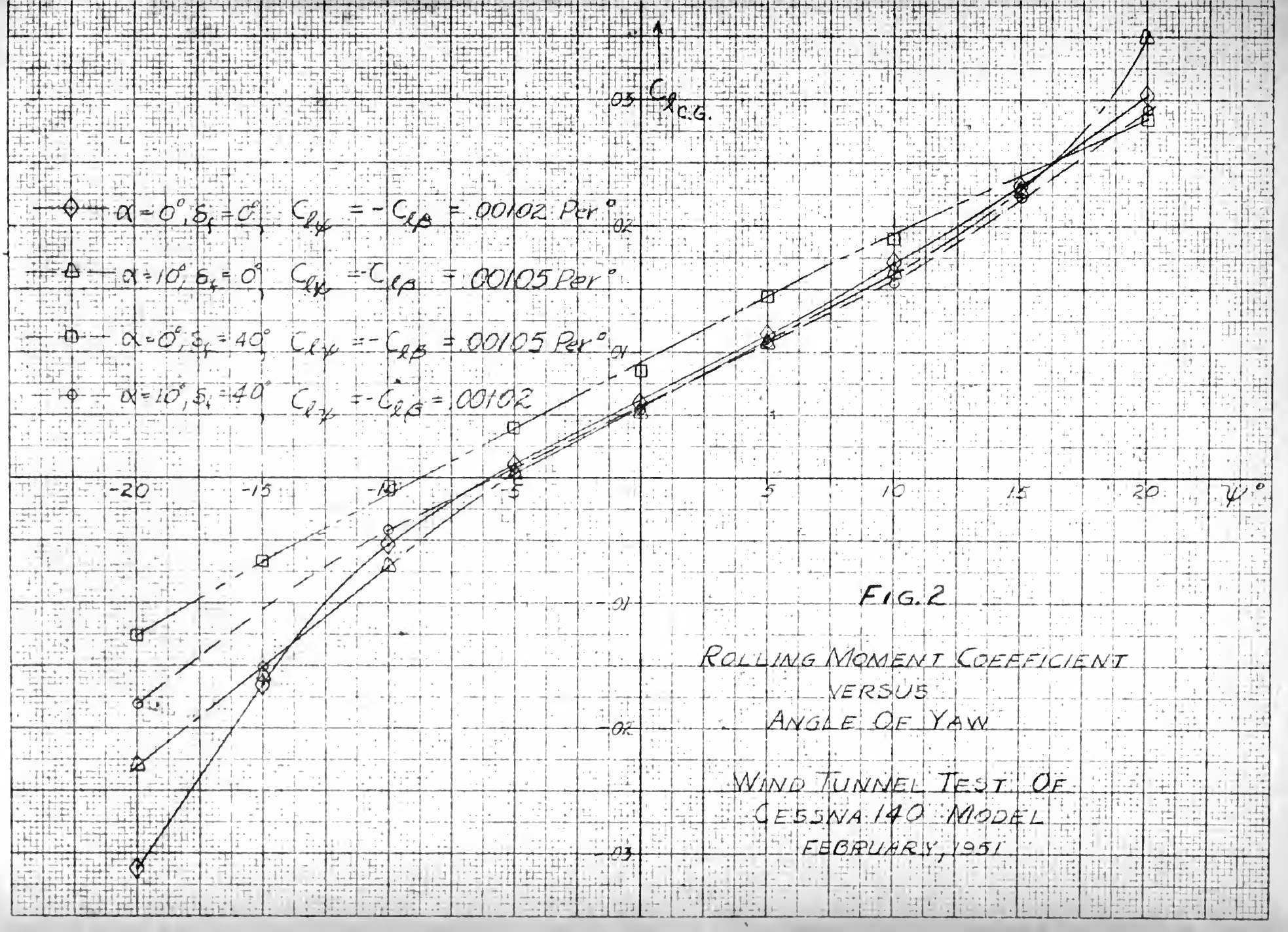

FIG. 2

ROLLING MOMENT COEFFICIENT
VERSUS
ANGLE OF YAW

WIND TUNNEL TEST OF
CESSNA 140 MODEL
FEBRUARY, 1951

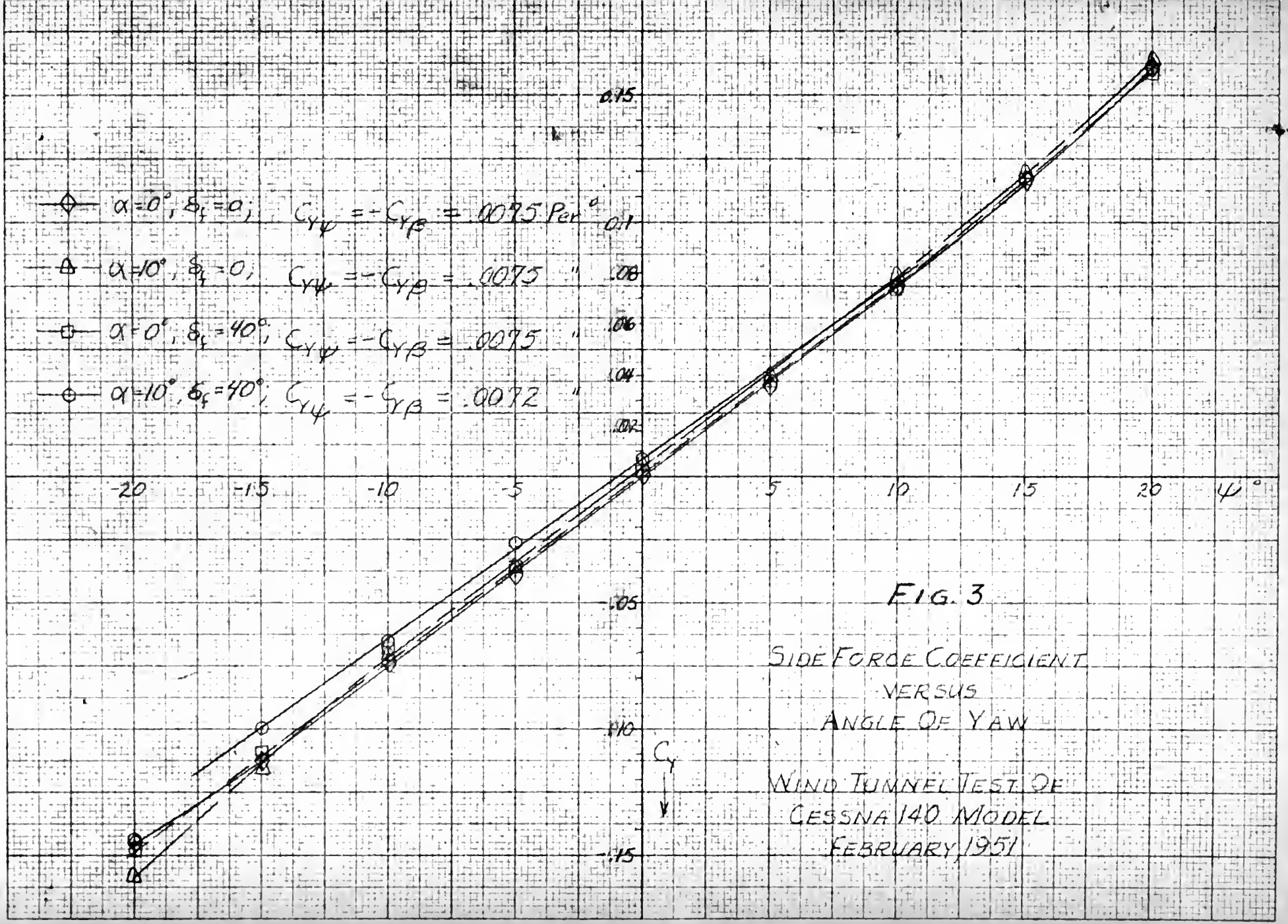

FIG. 3

SIDE FORCE COEFFICIENT
VERSUS
ANGLE OF YAW

WIND TUNNEL TEST OF
CESSNA 140 MODEL
FEBRUARY 1951

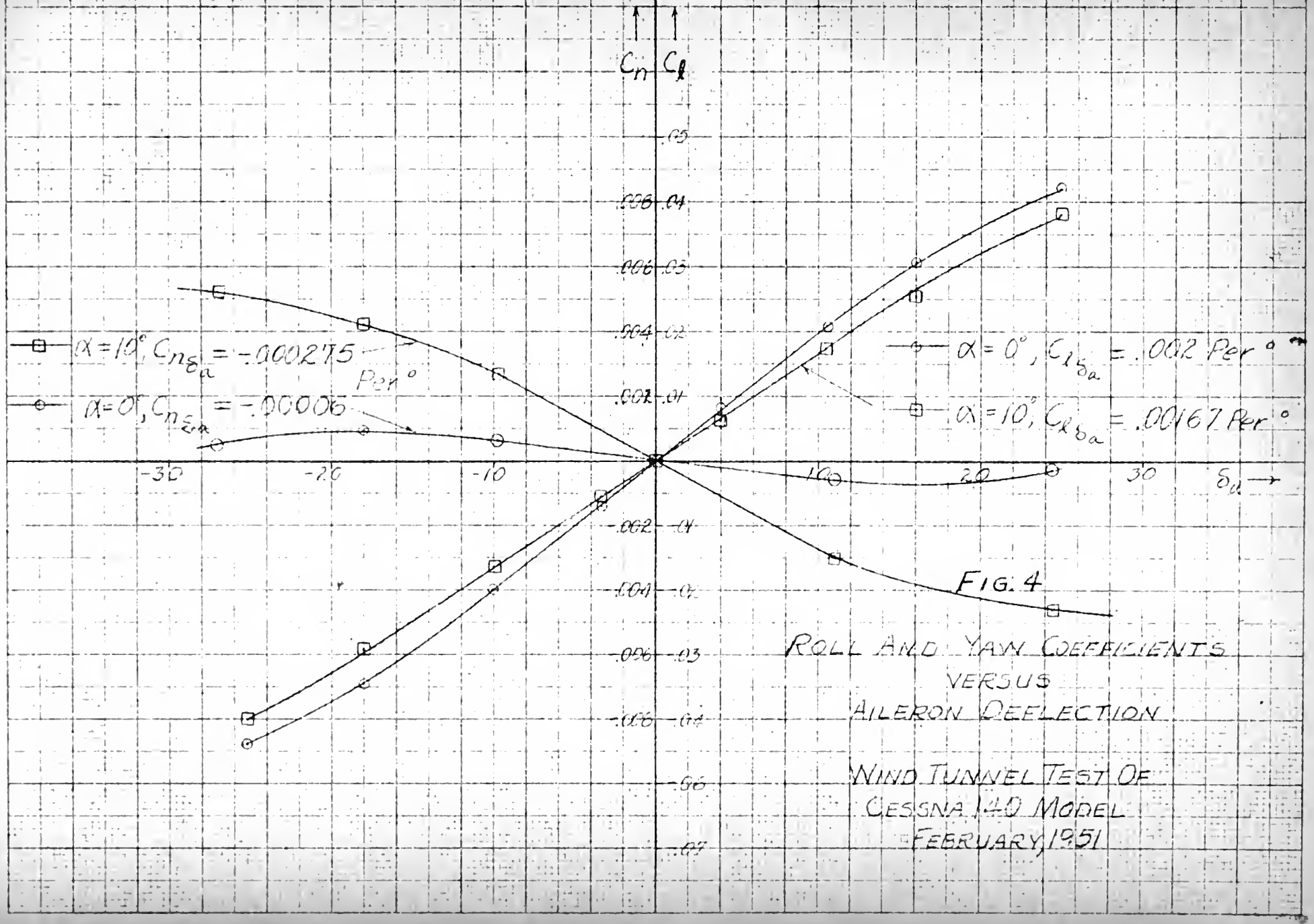

FIG. 4

ROLL AND YAW COEFFICIENTS
VERSUS
AILERON DEFLECTION

WIND TUNNEL TEST OF
CESSNA 140 MODEL
FEBRUARY, 1951

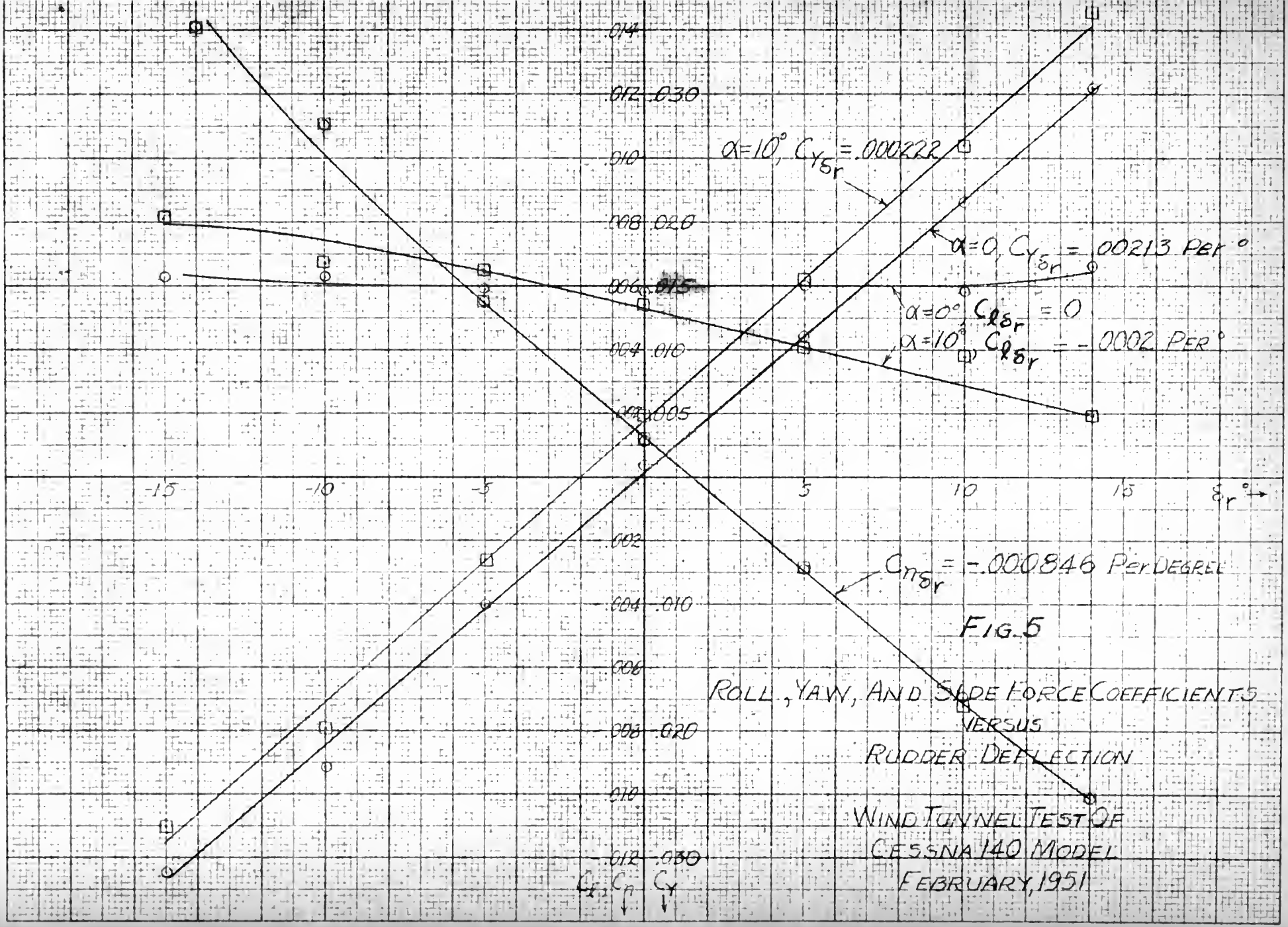

FIG. 5

ROLL, YAW, AND SIDE FORCE COEFFICIENTS VERSUS RUDDER DEFLECTION

WIND TUNNEL TEST OF CESSNA 140 MODEL

FEBRUARY, 1951

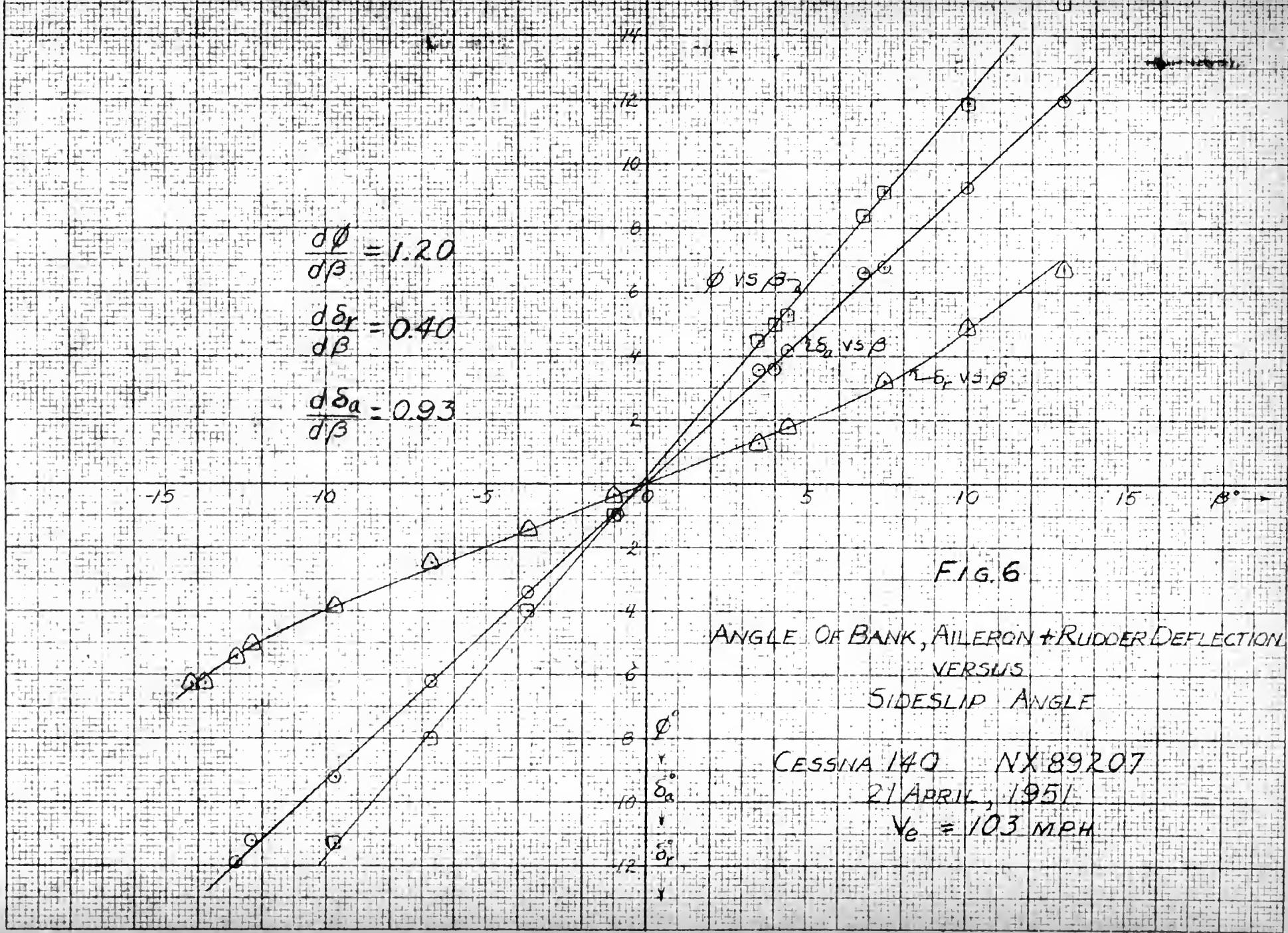

FIG. 6

ANGLE OF BANK, AILERON + RUDDER DEFLECTION
VERSUS
SIDESLIP ANGLE

CESSNA 140 NX 89207
21 APRIL, 1951
V_e = 103 MPH

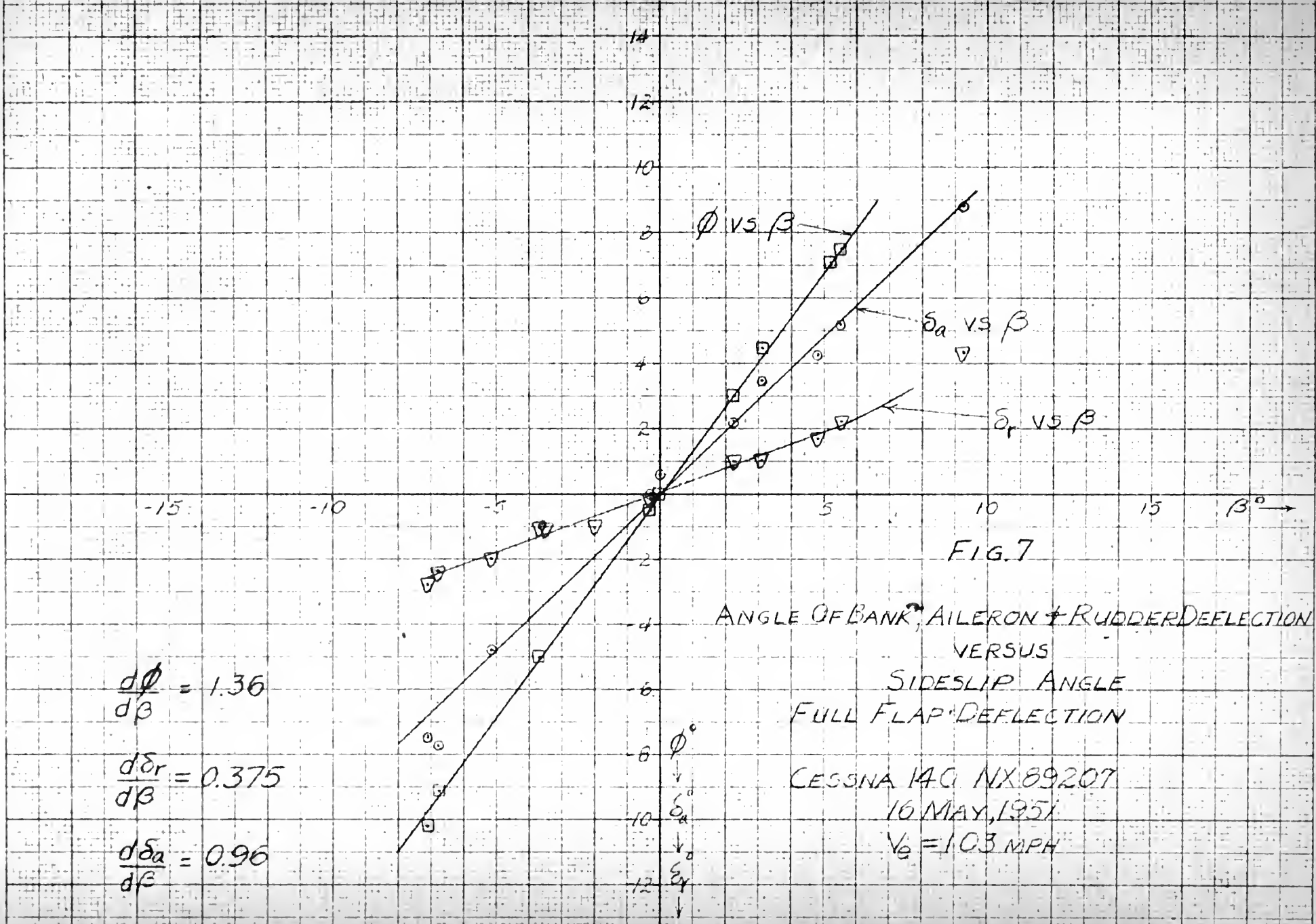

FIG. 7

ANGLE OF BANK, AILERON & RUDDER DEFLECTION
VERSUS
SIDESLIP ANGLE
FULL FLAP DEFLECTION

CESSNA 140 NX 89207
16 MAY, 1951
V_e = 103 MPH

$$\frac{d\phi}{d\beta} = 1.36$$

$$\frac{d\delta_r}{d\beta} = 0.375$$

$$\frac{d\delta_a}{d\beta} = 0.96$$

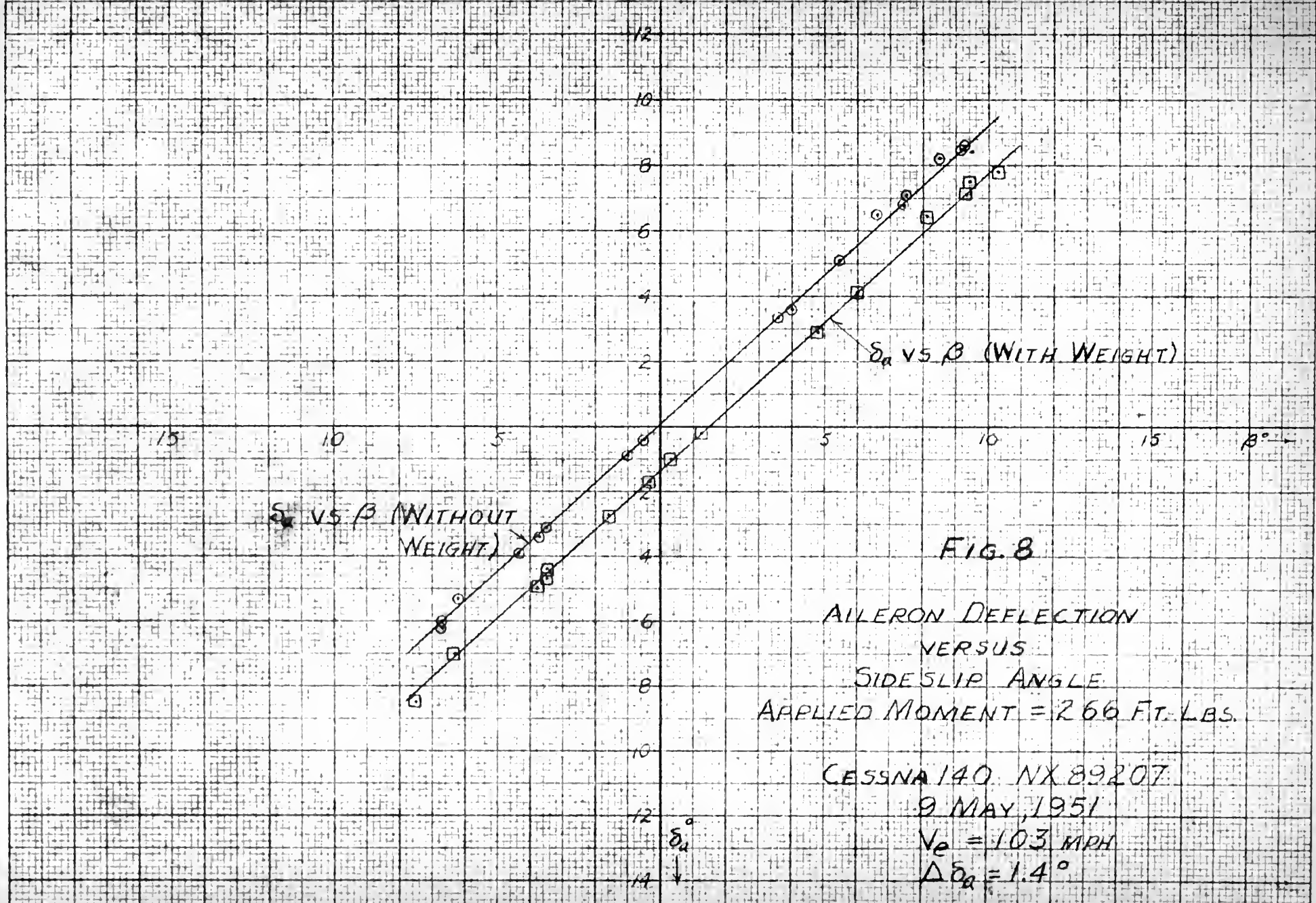

FIG. 8

AILERON DEFLECTION
VERSUS
SIDESLIP ANGLE
APPLIED MOMENT = 266 FT. LBS.

CESSNA 140 NX 89207
9 MAY, 1951
V_e = 103 MPH
$\Delta\delta_a$ = 1.4°

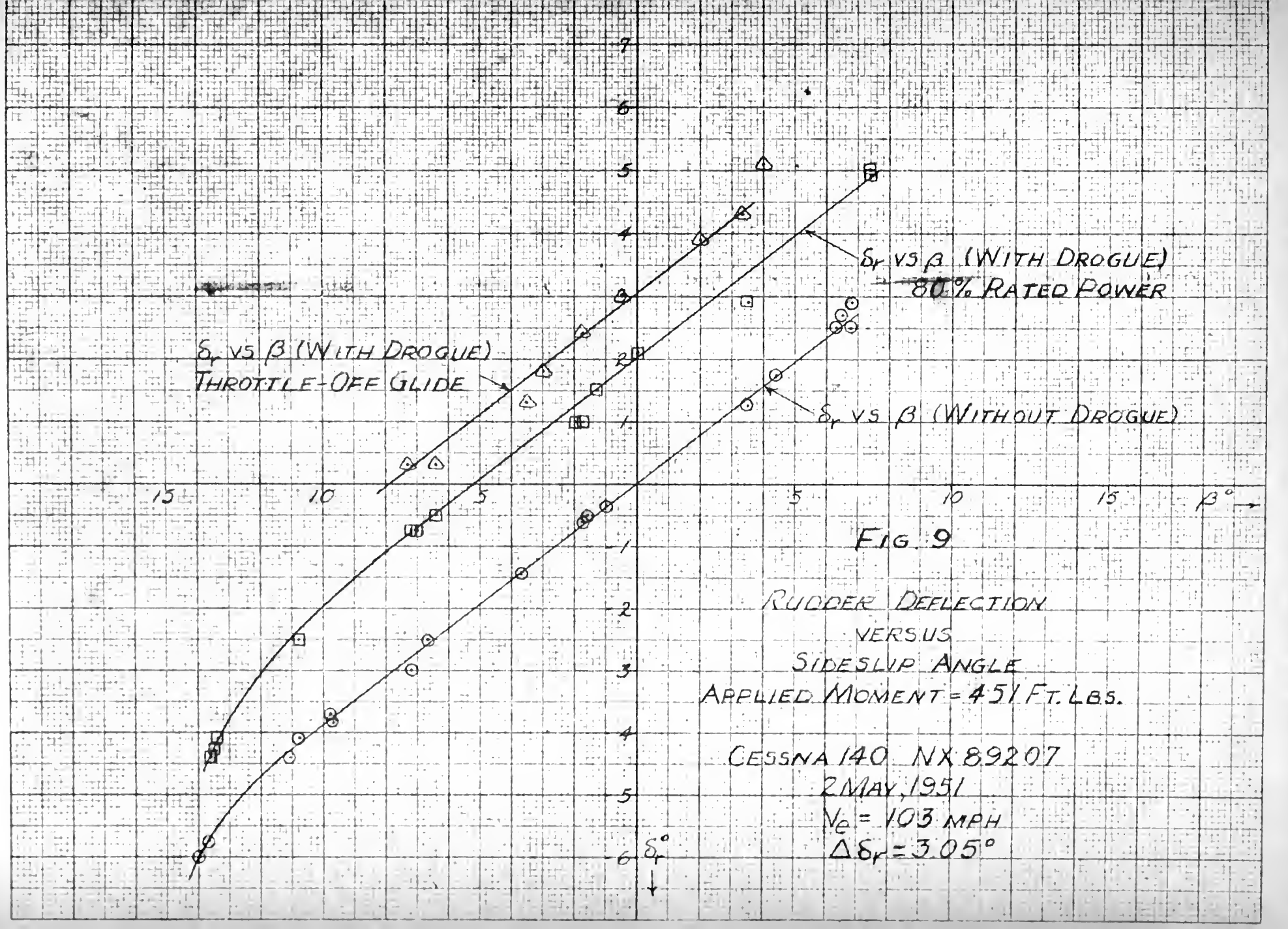

FIG. 9

RUDDER DEFLECTION
VERSUS
SIDESLIP ANGLE
APPLIED MOMENT = 451 FT. LBS.

CESSNA 140 NX 89207
2 MAY, 1951
V_e = 103 MPH
$\Delta\delta_r$ = 3.05°

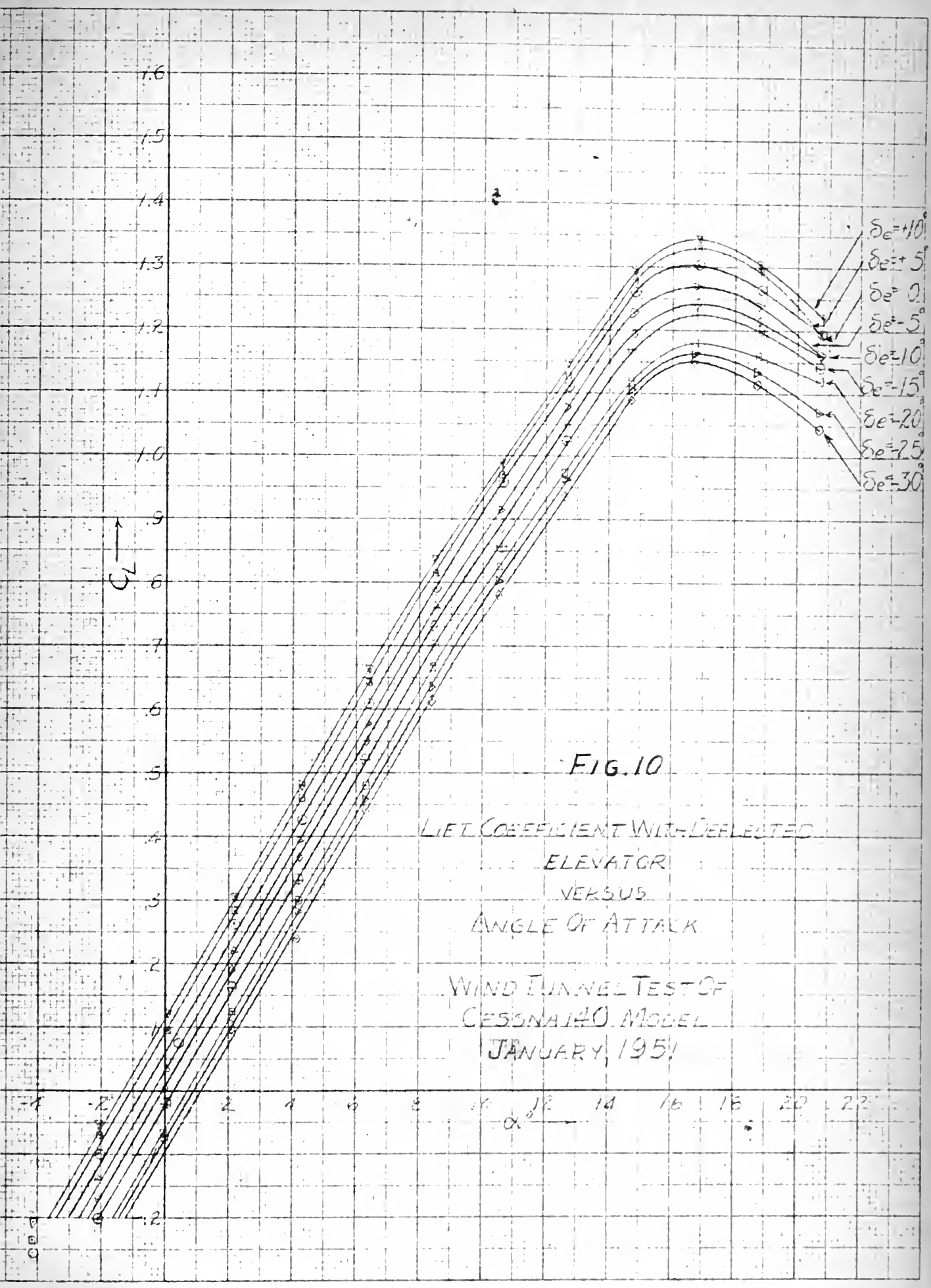

FIG. 10

LIFT COEFFICIENT WITH DEFLECTED ELEVATOR VERSUS ANGLE OF ATTACK

WIND TUNNEL TEST OF CESSNA 140 MODEL
JANUARY, 1951

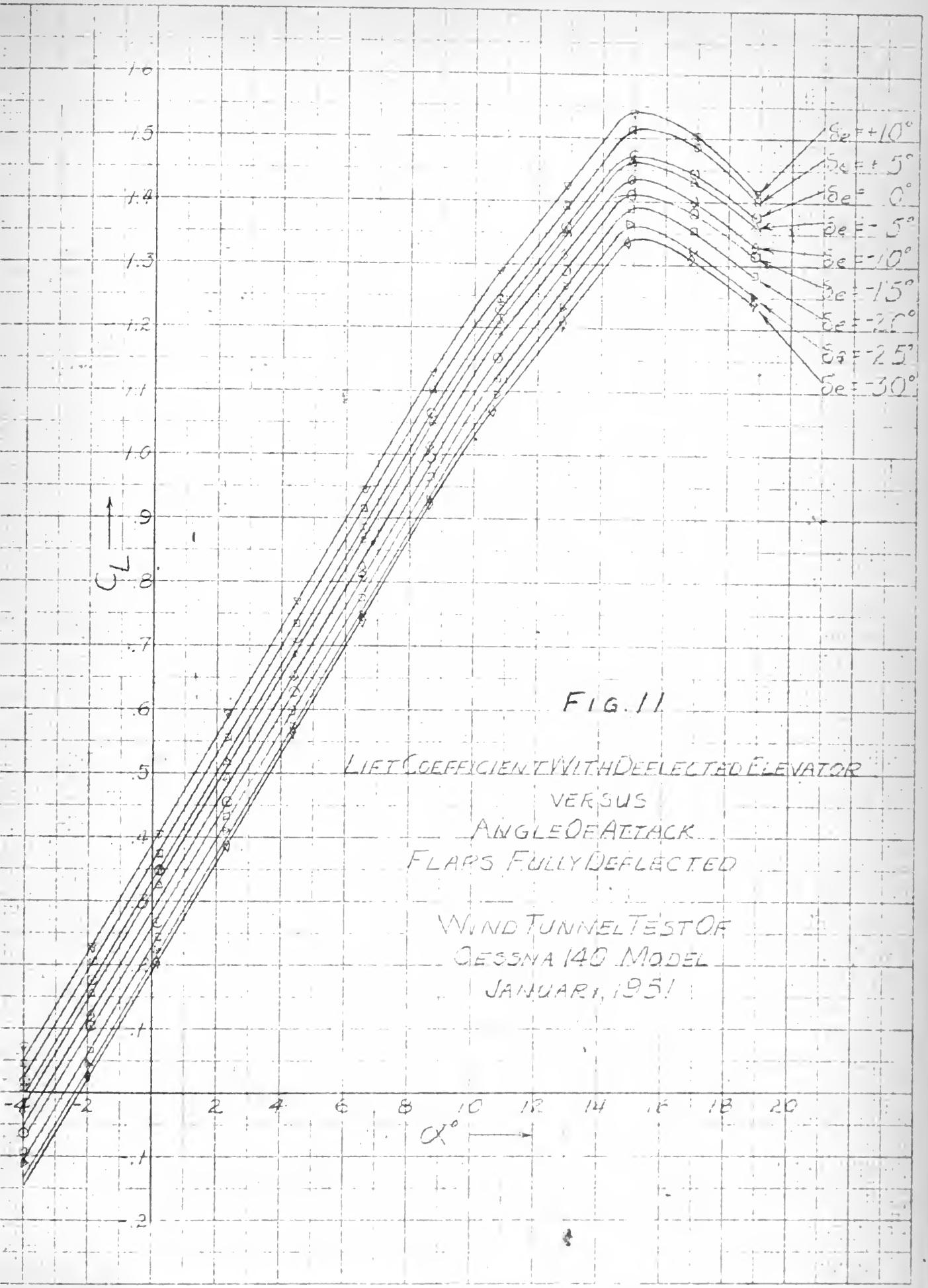

FIG. 11

LIFT COEFFICIENT WITH DEFLECTED ELEVATOR
VERSUS
ANGLE OF ATTACK
FLAPS FULLY DEFLECTED

WIND TUNNEL TEST OF
CESSNA 140 MODEL
JANUARY, 1951

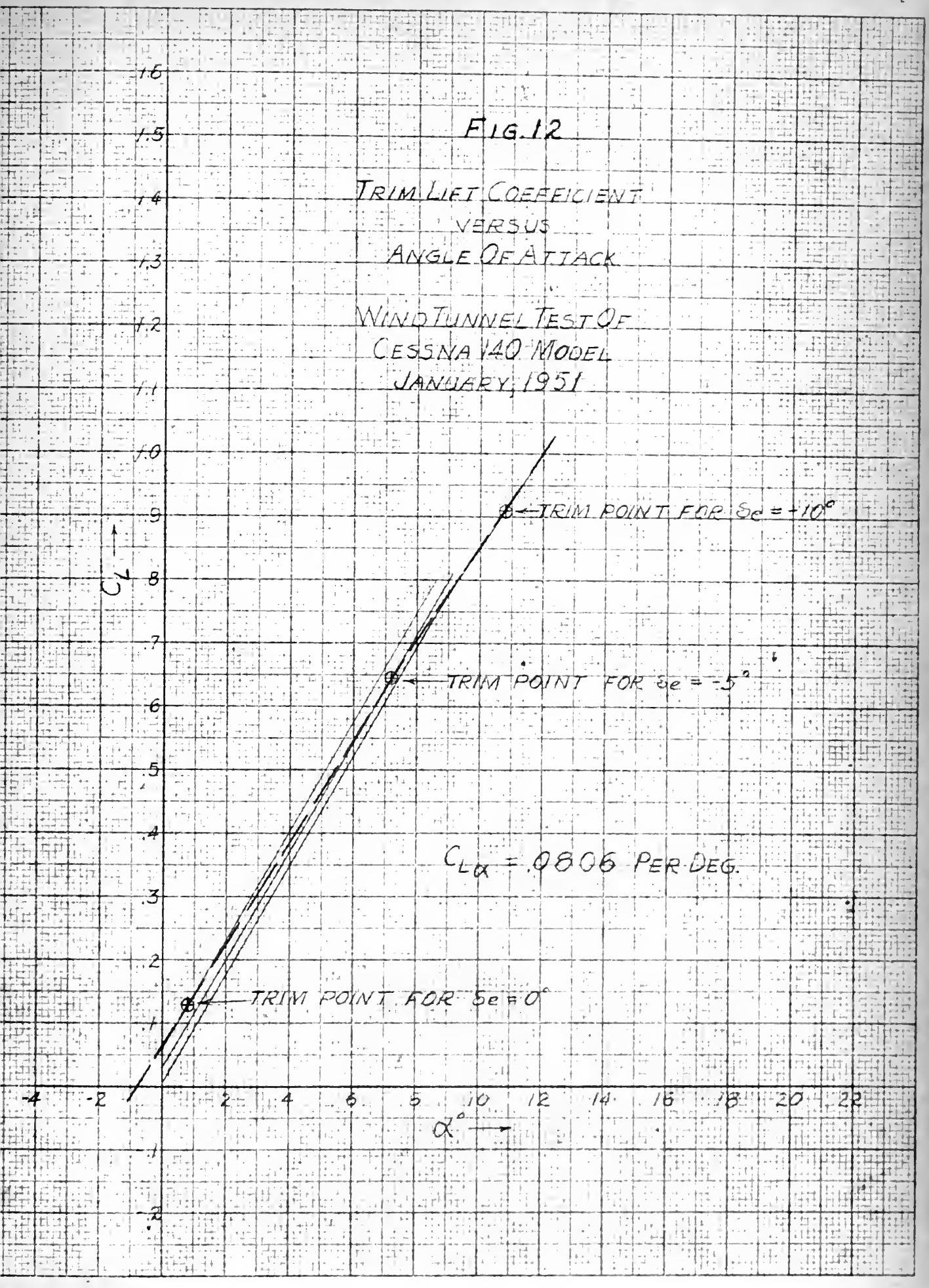
FIG. 12
TRIM LIFT COEFFICIENT
VERSUS
ANGLE OF ATTACK
WIND TUNNEL TEST OF
CESSNA 140 MODEL
JANUARY, 1951
TRIM POINT FOR δe = -10°
TRIM POINT FOR δe = -5°
TRIM POINT FOR δe = 0°
CLα = .0806 PER DEG.
CL
α°
1.6
1.5
1.4
1.3
1.2
1.1
1.0
.9
.8
.7
.6
.5
.4
.3
.2
.1
-.1
-.2
-4
-2
2
4
6
8
10
12
14
16
18
20
22

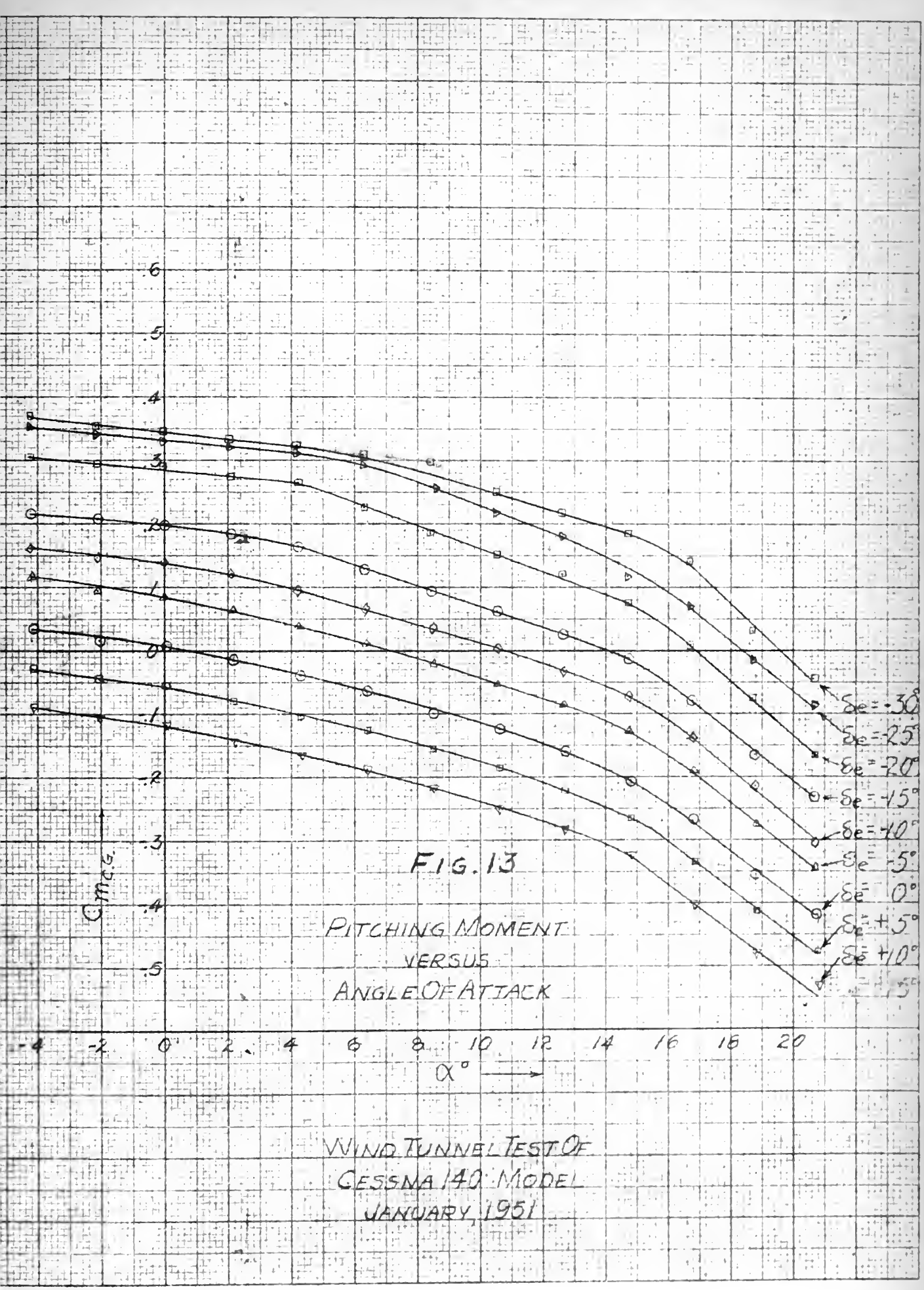

FIG. 13

PITCHING MOMENT
VERSUS
ANGLE OF ATTACK

WIND TUNNEL TEST OF
CESSNA 140 MODEL
JANUARY, 1951

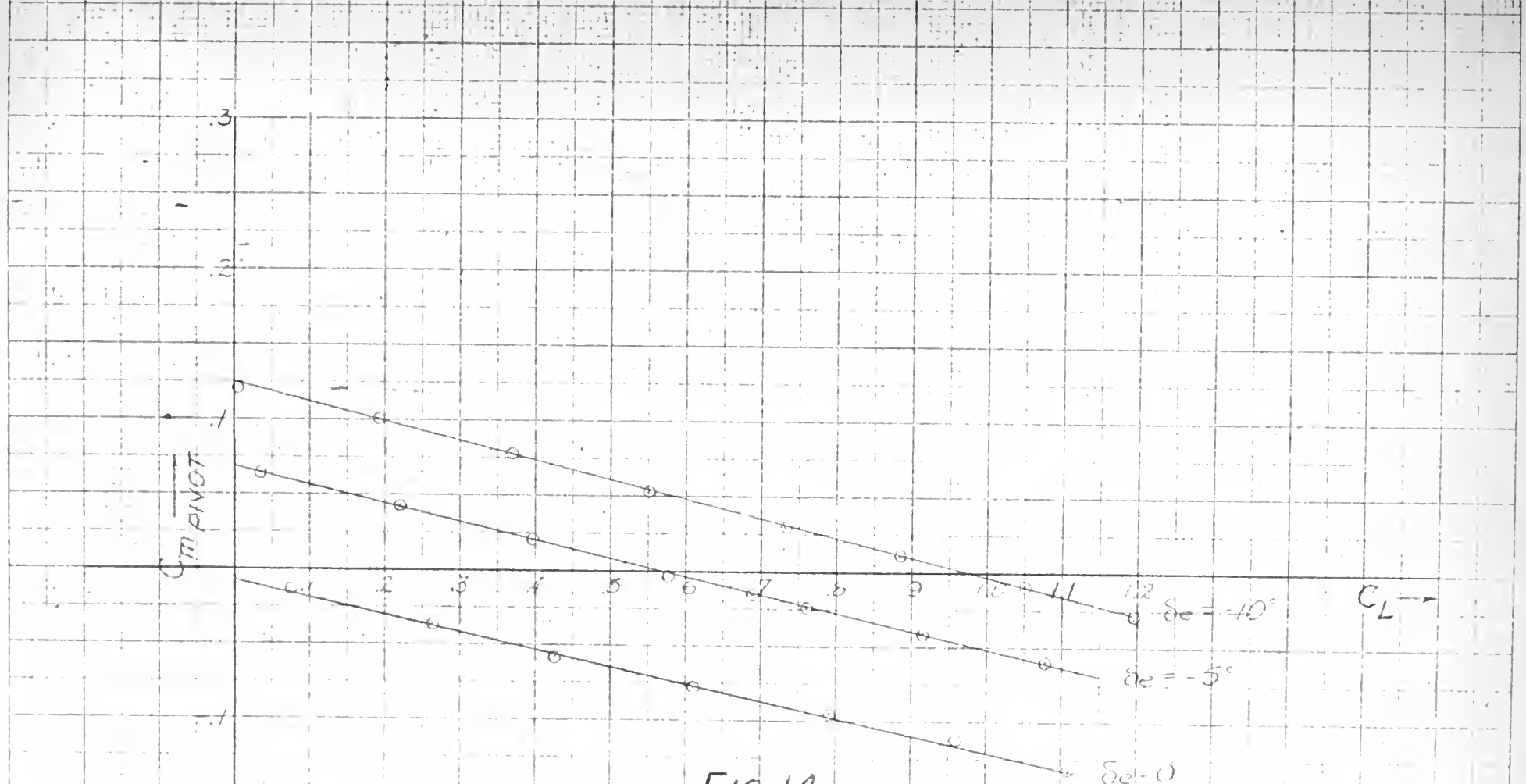

FIG. 14

PITCHING MOMENT
VERSUS
LIFT COEFFICIENT

WIND TUNNEL TEST OF CESSNA 140 MODEL
JANUARY, 1951

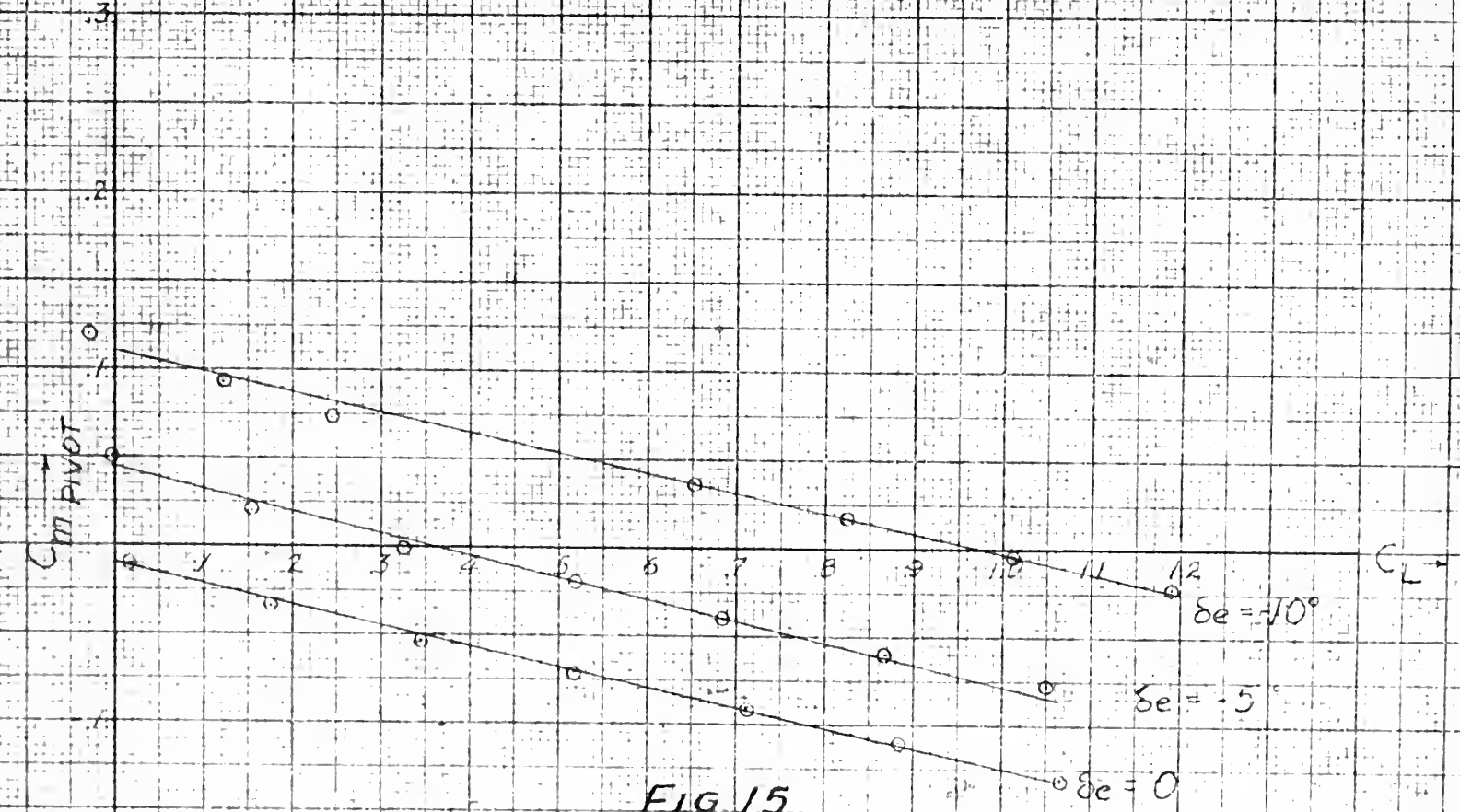

FIG 15

PITCHING MOMENT
VERSUS
LIFT COEFFICIENT
FLAPS FULLY DEFLECTED

WIND TUNNEL TEST OF CESSNA 140 MODEL
JANUARY, 1951

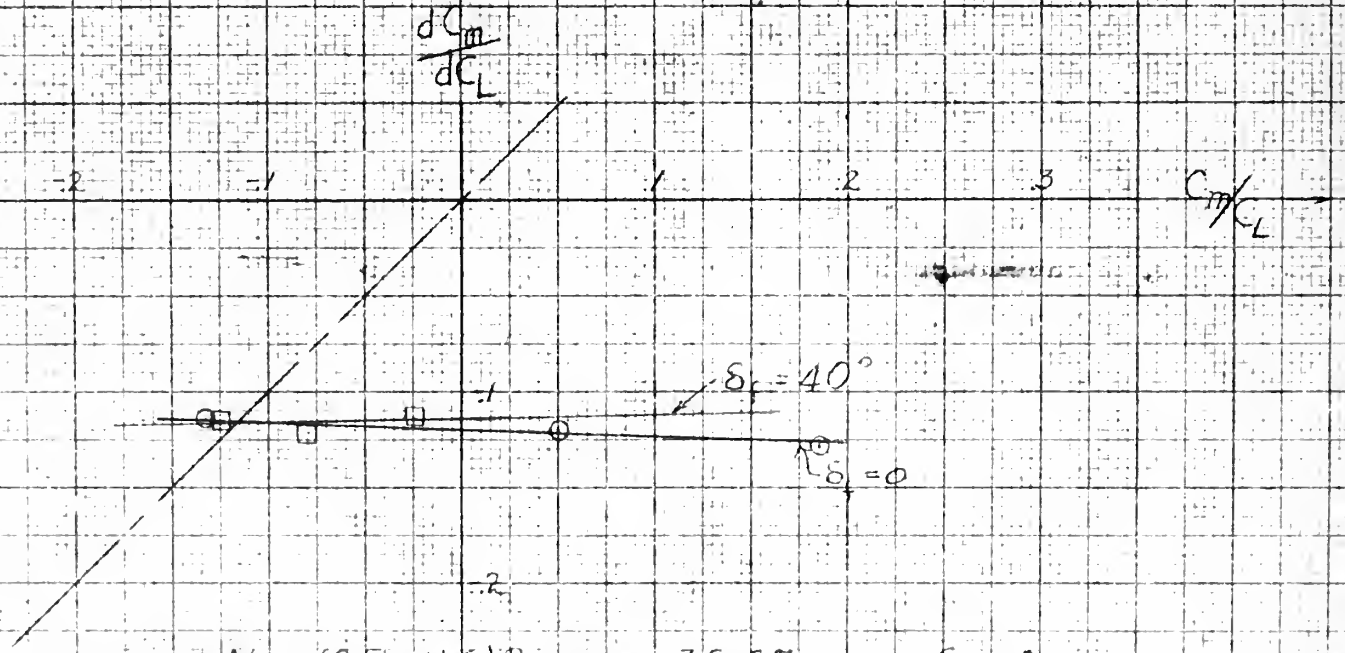

$N_o = (25 \pm 11.6)\%\ MAC = 36.6\%\ MAC$, $\delta_f = 0$

$N_o = (25 \pm 11.5)\%\ MAC = 36.5\%\ MAC$, $\delta_f = 40°$

FIG. 16

NEUTRAL POINT DETERMINATION
FROM
WIND TUNNEL TEST DATA ON
CESSNA 140 MODEL
JANUARY, 1951

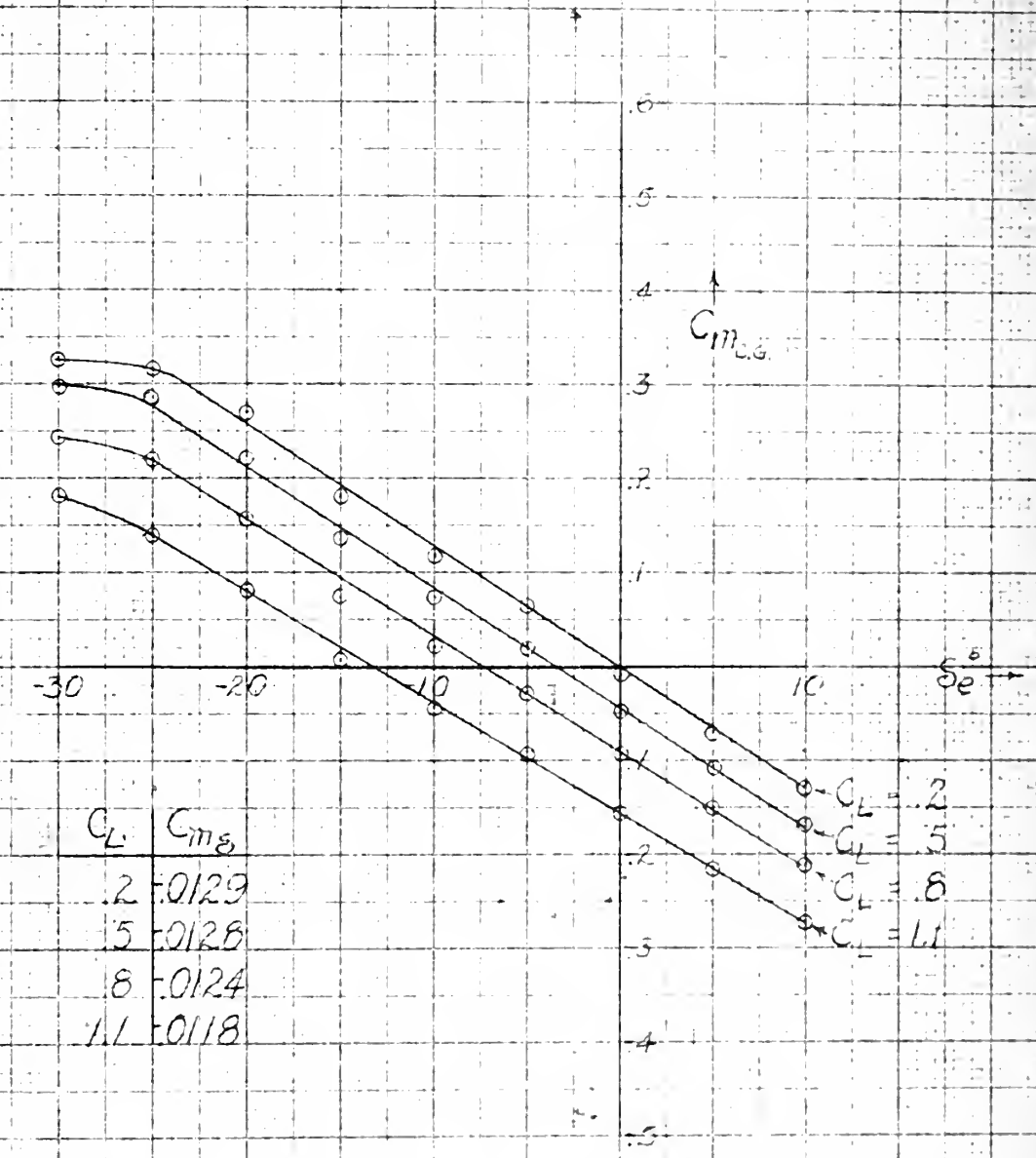

C_L	$C_{m_{\delta_e}}$
.2	-.0129
.5	-.0128
.8	-.0124
1.1	-.0118

FIG. 17

ELEVATOR POWER
FROM
WIND TUNNEL TEST DATA ON
CESSNA 140 MODEL
JANUARY, 1951

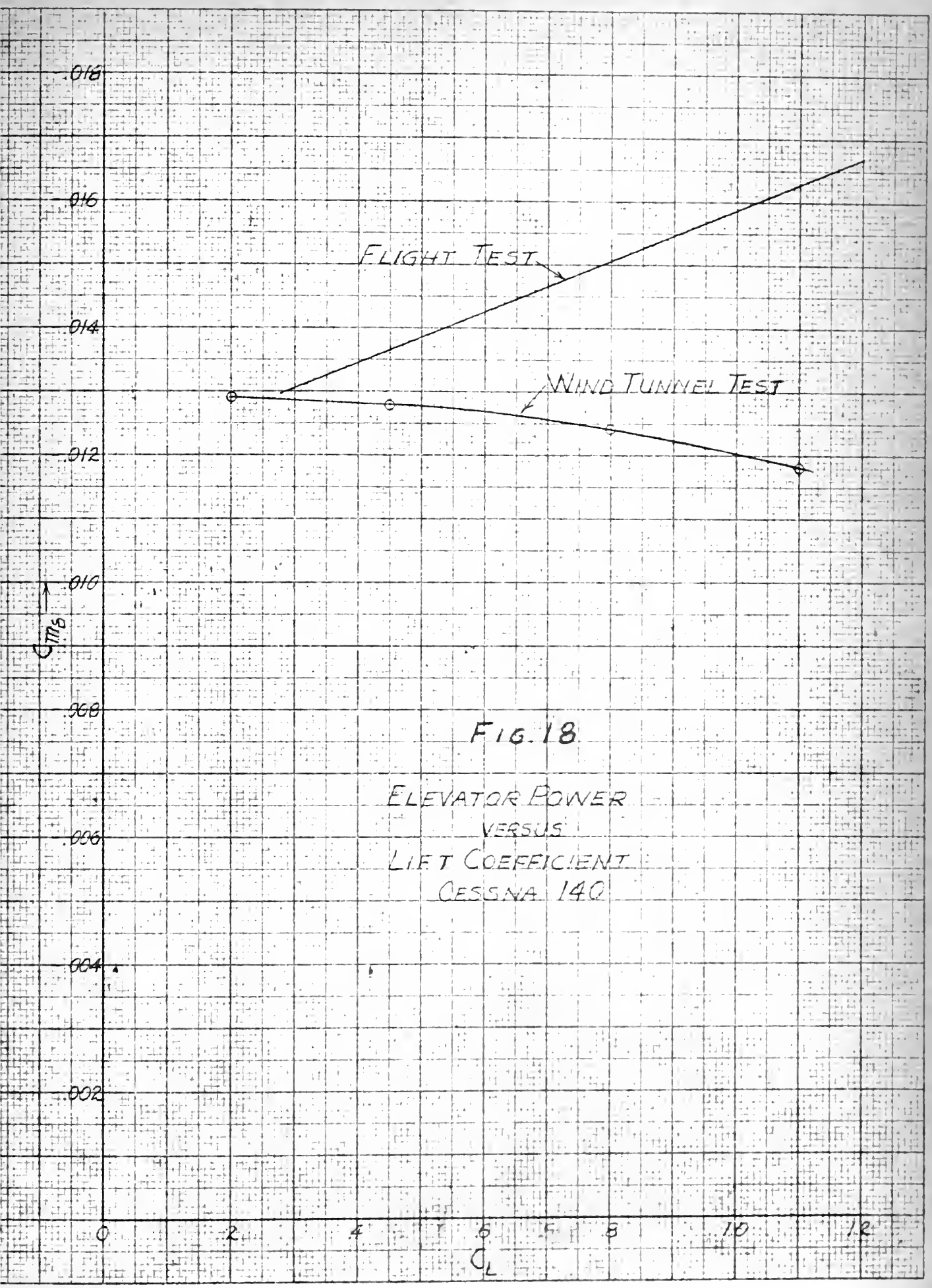

FIG. 18

ELEVATOR POWER
VERSUS
LIFT COEFFICIENT
CESSNA 140

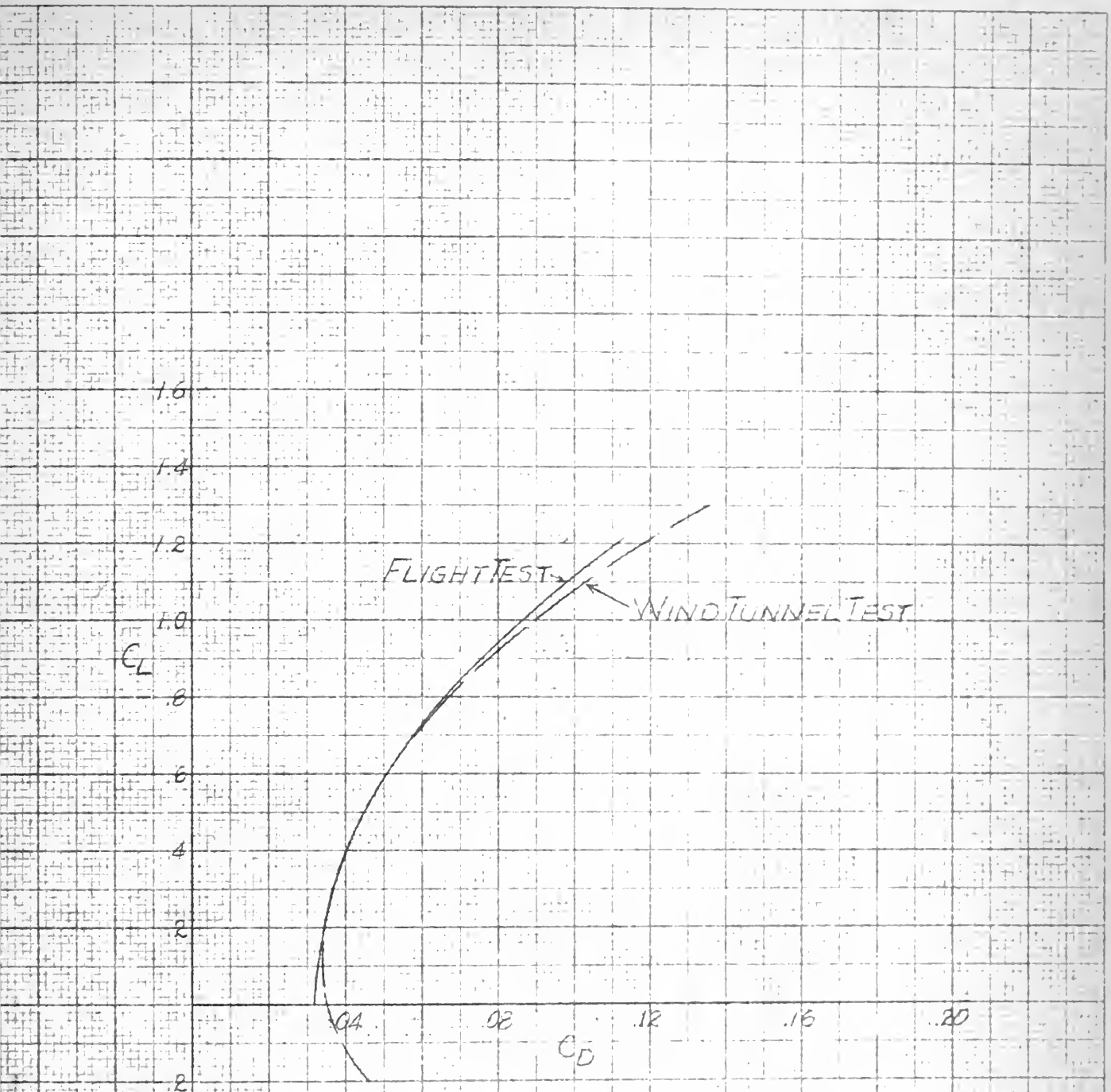

FIG. 19

DRAG POLAR COMPARISON
FIG. 14 - REF NO. 8

CESSNA 140

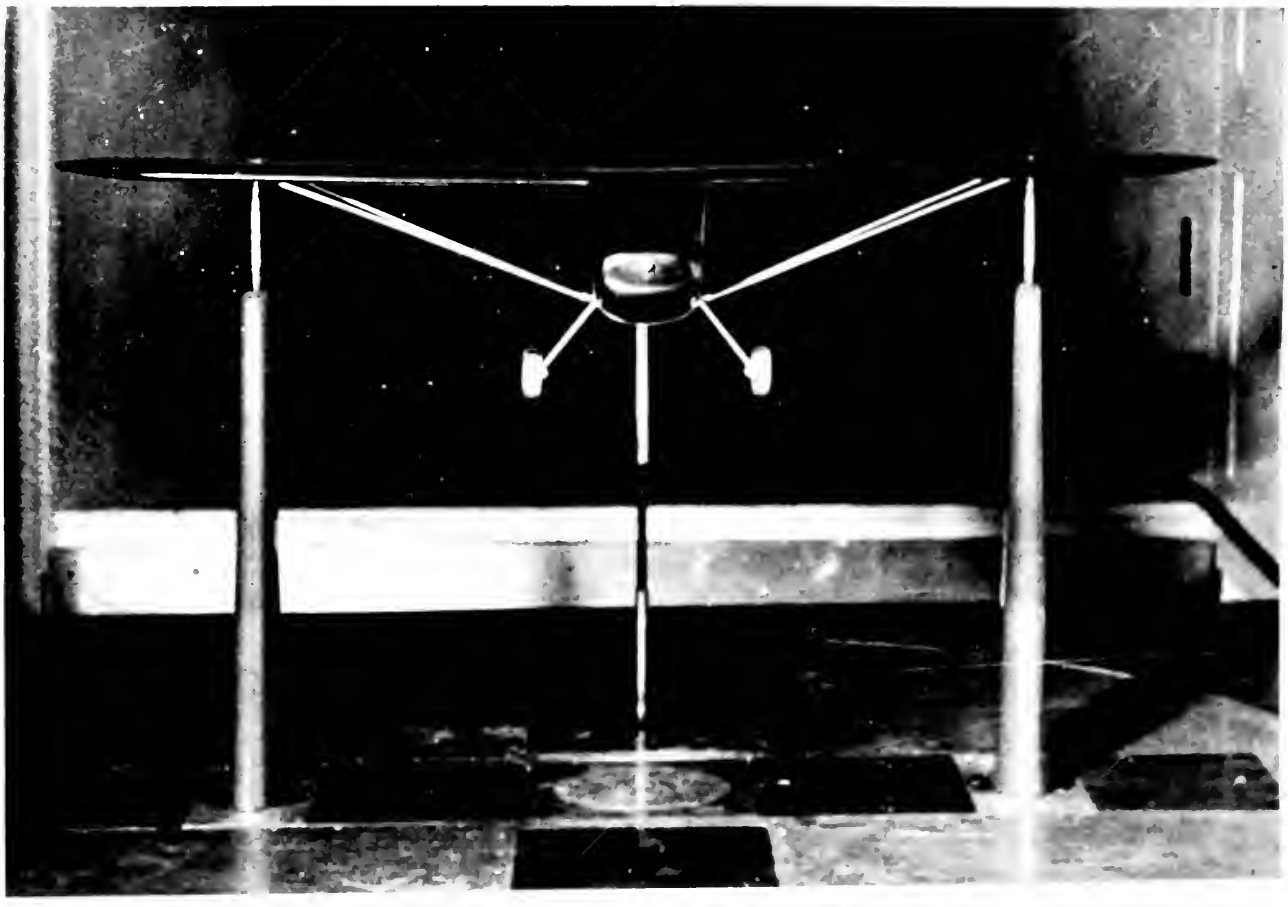

X APPENDIX I

Dimensions and description of Cessna 140 Airplane

Airplane General	
Manufacturer	Cessna Aircraft Co.
Type	140
Recommended gross weight	1450 lbs.
Center of gravity range	
forward limit	22.8 m.a.c.
aft limit	30.0% m.a.c.
Overall length	256.5 in.
Height	74.25 in.
Maximum allowable maneuvering load factor	
gross weight 1460 lbs.	4.57 to -2.26
flaps down 40°	1.97 to -2.26
Wing	
Airfoil section	NACA 2412
Span	394 inches
Area (total)	159.29 sq. ft.
Area (less ailerons)	145.21 sq. ft.
Aspect ratio	6.75
Taper ratio	1.0
Chord	60.5 inches
Mean aerodynamic chord	
Length	59.02 inches
Distance of leading edge back of nose reference datum line	56.58 inches
Incidence	1°
Dihedral	1°

Aileron	
Type	Modified Frieze
Area	14.08 sq. ft.
Span	74 inches
Chord	14 inches
Travel	
Up (from neutral)	22°
Down (from neutral)	14°
Wing flaps	
Type	Plain, trailing edge
Area	8.736 sq. ft.
Span	78.625 inches
Chord	8.0 inches
Travel (down)	40°
Horizontal Tail Surface	
Airfoil section	NACA 0009
Area (including elevators)	24.35 sq. ft.
Span	106 inches
Maximum chord	41.4 inches
Incidence	-2.5°
Dihedral	0
Elevator area (total, including tab)	9.66 sq. ft.
Elevator span	106 inches
Elevator travel	
Up (from streamline with stabilizer)	20°
Down (from streamline with stabilizer)	20°

Elevator trim tab area	0.695 sq. ft.
Elevator trim tab span	36 inches
Elevator trim tab mean chord	5.20 inches
Elevator trim tab travel	
Up (from elevator trailing edge)	6°
Down (from elevator trailing edge)	33°
Vertical tail surface	
Area	12.42 sq. ft.
Fin area	6.668 sq. ft.
Span (to fuselage center line)	52.2 inches
Rudder area	5.752 sq. ft.
Rudder span (maximum)	49.5 inches
Rudder travel	
Right (from streamline with fin)	16°
Left (from streamline with fin)	16°
Fuselage	
Maximum width	40.0 inches
Maximum height	51.0 inches
Length (tip of nose to tip of tail)	256.5 inches
Engine (Continental)	
Type	C 85
Number of Cylinders	4
Propeller	
Manufacturer	Flottorp
Type	Wood, fixed pitch
Diameter	74 inches

16268

Thesis B79 Boyd
. Wind tunnel and flight test information of the Cessna 140 for correlation of aerodynamic derivatives.